博士論文

Creation of surface-grafted gels and evaluation of skin layer formation ability

(表面グラフトゲルの創製およびスキン層形成能の評価)

松川　滉

Referee in chief:	Professor	Dr. Ryo Yoshida
Referee:	Professor	Dr. Kazuhiko Ishihara
	Associate Professor	Dr. Toshiya Sakata
	Associate Professor	Dr. Takamasa Sakai
	Lecturer	Dr. Aya Mizutani Akimoto

Acknowledgement

The present doctoral dissertation is the completion of works carried out at The University of Tokyo from April 2015 through March 2018 supervised by Professor Dr. Ryo Yoshida and Lecturer Dr. Aya Mizutani Akimoto at Department of Materials Engineering, School of Engineering, The University of Tokyo.

First of all, the author would like to express the deepest appreciation to Professor Dr. Ryo Yoshida for kindly welcoming the author as a member of his research group for six years, giving him persistent guidance and insightful suggestions, and giving him opportunities to attend domestic and international conferences and to collaborate with other institutes with financial supports. Thanks to them, the author could acquire precious experiences, knowledges, and a philosophy. They will powerfully help the author wherever he goes.

The author would also like to express the deepest gratitude to Lecturer Dr. Aya Mizutani Akimoto for her tolerant discussions and warm encouragements. Thanks to her, the author was able to endure the painful tasks, endeavor the continuous researches, and enjoy the life in the laboratory.

The author would like to express his gratitude to Dr. Yo Tanaka and Dr. Nobuyuki Tanaka at RIKEN for kindly offering the author the chance of collaboration and giving extensive discussions. The author repents not being able to spending so much time for the experiments of the collaboration.

The author would also like to express his gratitude to Professor Dr. Anna Christina Balazs at University of Pittsburgh for kindly accepting him in her

laboratory in summer 2016, and to her, Dr. Victor Yashin, Dr. Santidan Biswas, and Dr. Awaneesh Singh for their persistent guidances and valuable advices.

The author would also like to express his gratitude to Professor Dr. Kazuhiko Ishihara, Associate Professor Dr. Toshiya Sakata, and Associate Professor Dr. Takamasa Sakai for their extensive discussions and valuable advices.

The author would also like to express his gratitude to Professor Dr. Takuzo Aida for kindly letting the author to use the instruments in his laboratory.

The author would like to express his gratitude to Dr. Takeshi Ueki for his continuous guidance and valuable advices.

The author would like to express his gratitude to Dr. Tsukuru Masuda for his continuous guidance (from junior high school!!), valuable advices, and the collaboration work with the author. The author also deeply appreciates him for having lunch with him every day to Yamate-Ramen and Ichiban-Gyoza.

The author appreciates Mr. Hiroto Tada and Ms. Mari Yokozawa for the happy time and sometimes valuable advices and guidances. The author wishes to keep strong friendship with them forever. The author also appreciates Dr. Youn Soo Kim, Mr. Kenta Homma, Ms. Erika Hasuike Niitsu, Mr. Taipei Nishimoto and Ms. Mami Furusawa for their collaboration works with the author. The author also appreciates Dr. Yusuke Shiraki, Mr. Satoru Kunikata, Ms. Lilian Hikaru Shido, Ms. Kaori Bundo Suzuki, Mr. Reo Mitsunaga, Mr. Kazuma Ebina for their cheerful advices, and Mr. Eun Jong Lee, Ms. Catherine Shasteen, Mr. Michika Onoda. and all the other members in Yoshida-Akimoto Laboratory for the great time in the laboratory and others.

The author gratefully appreciates his fiancée, Ms. Risa Matsui for all her supports. Thanks to her, the author was able to do his best without any worry.

The author deeply appreciates Materials Education program for the future leaders in Research, Industry, and Technology (MERIT) for the financial support and the offer of opportunities of interactions with professors (especially with Professor Dr. Akira Toriumi) and students in materials field.

Last, but not least, the author feels greatest gratitude to his family for raising and supporting him until now, especially during his student life for more than 20 years! From now, in turn, the author would like to repay their kindness.

Ko Matsukawa

Department of Materials Engineering

School of Engineering

The University of Tokyo

March 2017

Table of Contents

Chapter 1:
General introduction

1-1. Background

1-1-1. Biomimetic materials / bioinspired materials

We, human beings, have accumulated the knowledge of science during the history, and have tried to understand the basic principles of cosmos and to create the novel functional materials which will enhance the quality of our lives. On the other hand, animals and plants have gained the splendid and complex functions during much longer history. From this view point, they are always the pioneers of science. Recently, as a cutoff to gain such splendid and complex functions, there are many researches which try to imitate the designs of animals and plants, or to evolve superior functions inspired from them, so-called "biomimetic materials" or "bioinspired materials."[1] This kind of researches range from zero-dimensional molecules to three-dimensional structures. As an example of biomimetic molecules, a catecholic binder inspired from the adhesive protein of bivalves can be raised.[2] Mussels, which live under the sea with adhesion to rocks, are known to secrete a peptide which includes 3,4-dihydroxy-L-phenylalanine (DOPA) from their byssuses. By focusing on the catecholic structure which DOPA has and synthesizing a polymer with this chemical structure in side chains, a new binder was developed which strongly binds materials non-specifically in water with high ion strength.

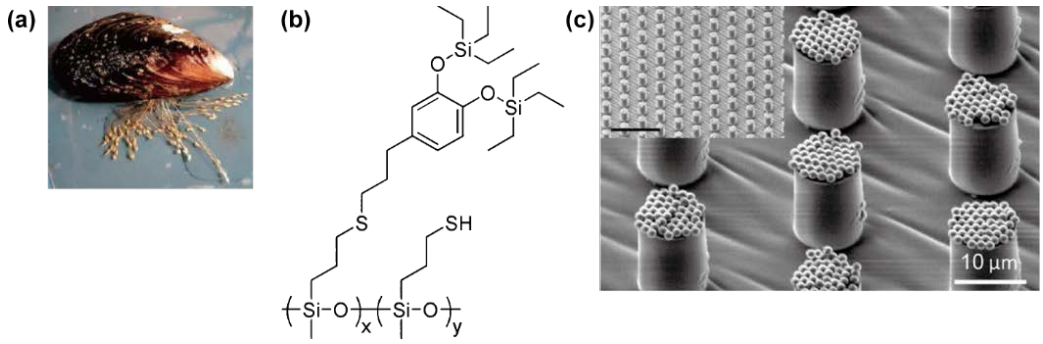

Figure 1-1. (a) Picture of Mussel. Yellow filiform organ is byssus. (b) Chemical structure of bioinspired silyl-protected catechol (SPC)-functionalized polysiloxane. (c) Pillar-shape substrates composed of SPC-functionalized polysiloxane. Silica particles strongly adhere the top of the pillar.[2]

Then, as an example of biomimetic structure, a painless needle which imitates the structure of mosquito's proboscis can be raised.[3] This needle is composed of three tiny needle as mosquito's one; the center of them is electro-chemically etched into three-dimensionally sharp shape with finely smooth surface, and outer two needles are machined into jagged shank shape by a deep reactive ion etching (DRIE). This complex structure enables to lower the possibility to stimulate the pain points during penetration of skin, resulting in "painless."

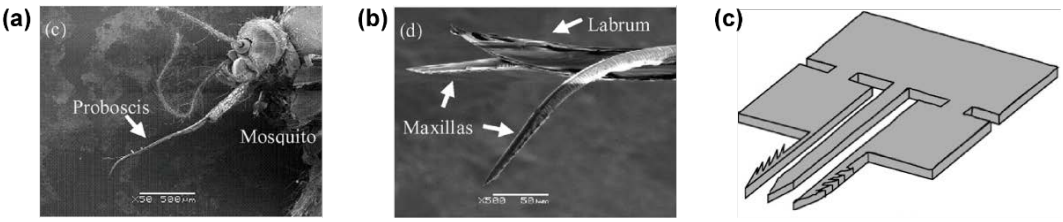

Figure 1-2. (a), (b) Images by optical microscopy of mosquito's proboscis composed of several separated needles. (c) Schematic image of biomimetic needle composed of three needles fabricated by DRIE.[3]

Super-hydrophobic surface which imitates the surface structure of lotus leaves is also a good example of biomimetic materials.[4] The surface of lotus leaves has hierarchical micro- and nano-ordered structure, which lower the contact area with water droplets. Reproducing this unique structure by treating the surface of aluminum alloy using sodium hydroxide and subsequently spin-coating perfluorononane or poly(dimethylsiloxane) leads to artificial super-hydrophobic surface.

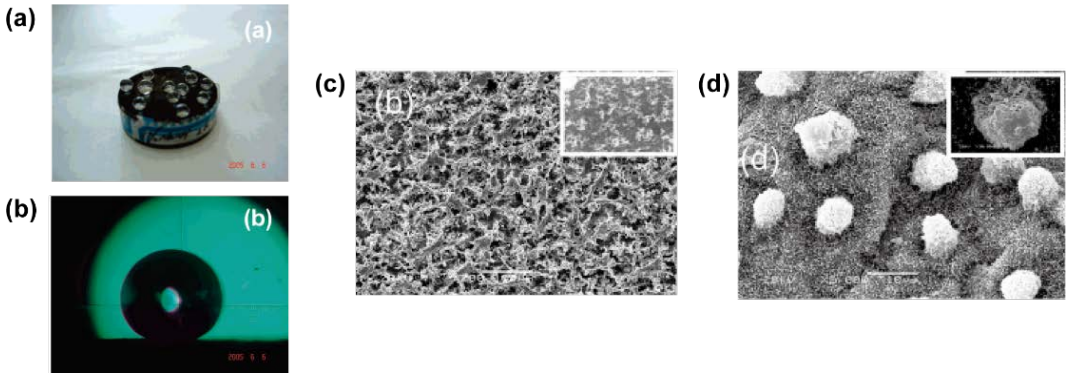

Figure 1-3. (a), (b) Image of superhydrophobic surface of aluminum surface treated with NaOH and coated with C_9F_{20}. (c), (d) SEM images of the surface of the treated aluminum alloy and lotus leaf, respectively. The insets are taken with larger maginification.[4]

In addition, there are also many spatio-temporally ordered functions in nature driven by dissipative structure which can be observed in non-equilibrium open system. Benard conviction, which causes the pattern of cirrocumulus cloud, and Turing pattern, which is observed in the pattern of animal skin such as zebra fish,[5] are the typical examples for that. It is also possible to create spatio-temporally ordered structure using only artificial materials.

Belousov-Zhabotinsky (BZ) reaction, which is one of the chemical oscillating reaction and known to have analogy to an *in vivo* metabolic cycle, TCA cycle, shows a periodic change of the charge of catalytic metal ion complex in presence of appropriate concentration of strong acid (nitric acid or sulfonic acid), oxidant (sodium bromate) and reductant (malonic acid).[6] In addition, BZ reaction also shows a unique pattern with the propagation of chemical waves when the reaction system is two-dimensionally wide by impregnating filter paper with reaction solution.

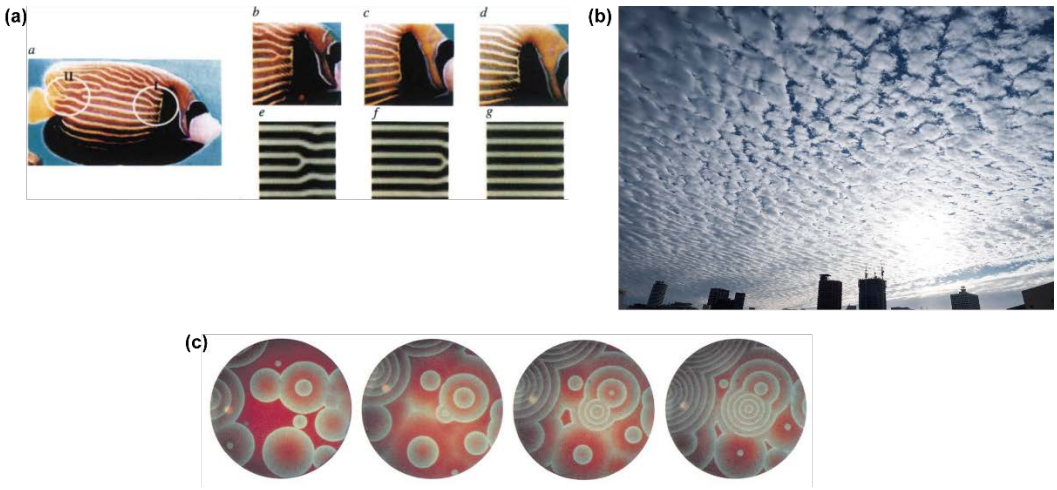

Figure 1-5. (a) Stripe pattern of zebra fish and its time evolution, which corresponds well to computer simulation based on the idea of Turing pattern.[5] (b) Picture of cirrocumulus cloud. (c) Time evolution of the pattern of chemical wave of BZ reaction.[6]

Furthermore, by incorporating BZ reaction into thermoresponsive hydrogels; synthesizing the hydrogel which composed of thermoresponsive polymer, poly(N-isopropylacrylamide) (PNIPAAm), copolymerized with ruthenium catalyst-derived monomer, Yoshida et al. developed the hydrogel which shows

autonomous volume change like heartbeat in the presence of BZ reaction substrates, so-called self-oscillating gel.[7],[8] Additional optimization of the shape also enables self-walking,[9] mass transport like conveyer belt,[10] and micropump.[11]

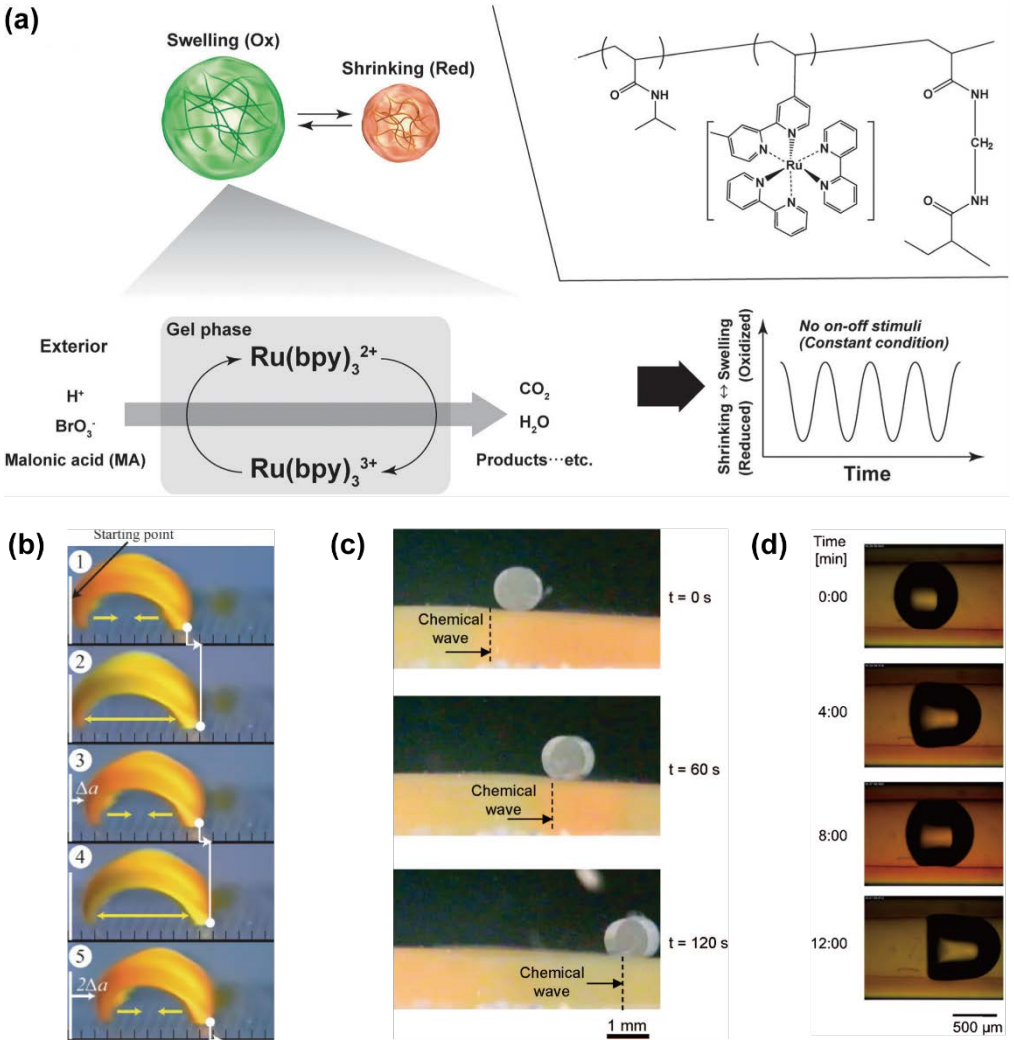

Figure 1-6. (a) Illustration of self-oscillating gel and its chemical structure.[8] (b), (c), (d) Pictures of self-walking gel,[9] autonomous mass transport of cylindrical hydrogel by sheet gel,[10] autonomous transport of CO_2 bubble by tubular gel,[11] respectively, driven by self-oscillation.

Metamorphosis is one of the most interesting phenomena observed in nature non-equilibrium system. It is because the time scale of metamorphosis ranges for months or years, and, especially in the case of complete metamorphosis, appearances and functions changes dramatically from juvenile worm form to adult form with wings through this phenomenon. Thanks to the advance in imaging technology, now metamorphosis can be observed in detail without dissection by high-resolution X-ray computed tomography (CT).[12] At the pupal stage, which is peculiar to complete metamorphosis, (i) the surface is covered by a hard shell and mass transport through the shell is limited, and (ii) the inside of the shell behaves as a reaction field where tissues except for tracheal system and nervous system are once solated and the reconstructed into adult tissues. Conversely, it can be said that imitating these two characteristics is necessary for achieving dramatic function change or change for long time scale using artificial materials. However, there have not been the researches which focuses on mimicking the metamorphosis. Here I focus on hydrogels with some reversible shells for creating artificial pupa or metamorphosis, because hydrogels have some physical properties close to living bodies such as open system, high water content, and elasticity.

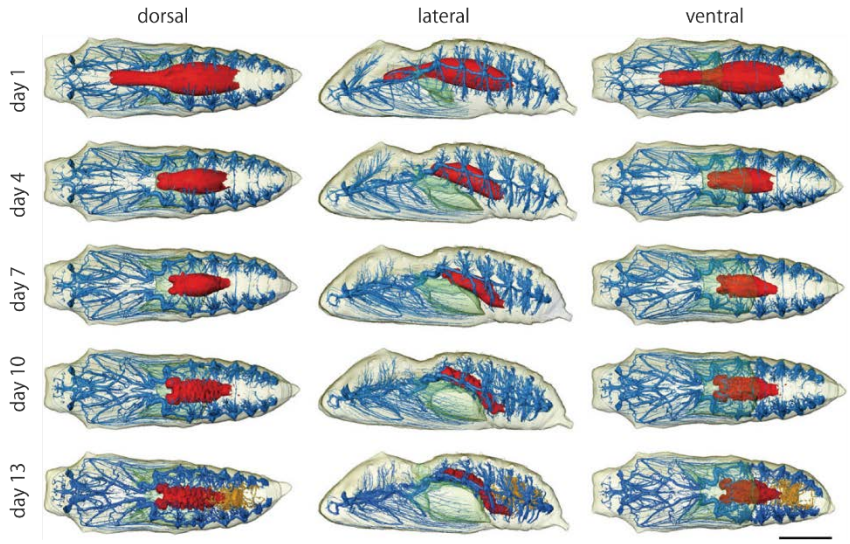

Figure 1-7. Pupal stage during metamorphosis observed by time-lapse CT-scanning. Tracheal system, midgut, Malpighian tubules, air lumen are shown in blue, red, orange, green, respectively.[12]

1-1-2. Skin layer

As mentioned above, hydrogels are open system materials, where physical and chemical signals easily enter and leave the polymer network. Since Tanaka et al. reported volume phase transition,[13] where hydrogels change their volume drastically in response to external stimuli including temperature, pH, light, there have been thousands of researches about application for soft actuator using this unique property.[14]-[19] It is known that shrinking and swelling of hydrogel proceed by cooperative diffusion and they start from the boundary of the gel system, i.e., the surface of the gel. Therefore, at the early stage of shrinkage, the polymer network only in the surface region shows the increase in polymer density and the inner keeps its original state. When the shrinking surface polymer

network gets dense enough to suppress the water permeation, the gel stops shrining and keep its volume. Here, this polymer-rich shrunken layer with several tens micrometer thickness is called “skin layer.” The state with the formation of skin layer can be recognized as reversible closed system because the mass transport through skin layer is strongly limited and once the external stimuli is removed the skin layer rapidly disappears, and seems to have analogy to the pupal state during metamorphosis. While skin layer is usually regarded as an evil which ruins the gels’ functionalities, there are also researches focusing on skin layer. Tanaka et al. reported unique shrinking patterns (bubble, bamboo. etc.) which are observed by keeping gels for a long time with the formation of skin layer, and confirmed that the patterns are dependent on the external condition and the shape of themselves.[20] It is because keeping the shape with skin layer is physically unstable and the gels try to reach most stable state where they shrink partly and swell in the neighbor region with the total volume constant.

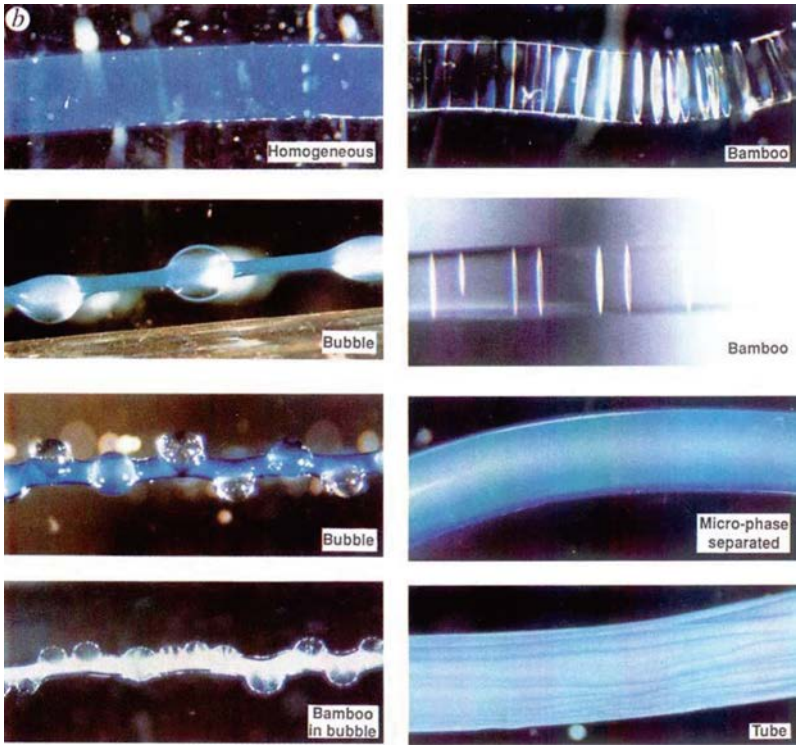

Figure 1-8. Shrinking pattern of polyacrylamide gels shrinking in acetone-water mixture. Pattern differs depending on the ratio of acetone and the relative length of gels.[20]

As an example of utilizing skin layer, Matsumoto et al. reported the controlled release of insulin molecules using the formation and deformation of skin layer.[21] They synthesized the hydrogels which composed of PNIPAAm copolymerized with phenylboronic acid-derived monomer. At the physiological temperature, this gel shrinks and forms skin layer without glucose, and swells in the high concentration glucose solution. Therefore, by loading insulin inside the gel, it only releases loaded insulin in response to high concentration of glucose with the deformation of skin layer.

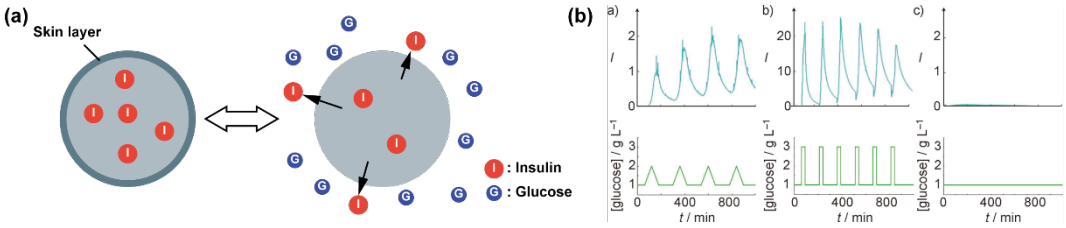

Figure 1-9. (a) Schematic image of insulin-releasing hydrogel controlled by glucose concentration. (b) Releasing profile of this gel depending on the change of glucose concentration.[21]

A problem of utilizing skin layer for application is the dependency of its formation on the composition of polymer network. As mentioned above, the condition that the permeability of shrunken surface polymer network gets extremely low in early stage of shrinkage is necessary for the formation of skin layer. For example, the polymer network is relatively hydrophilic, stable skin layer will not be formed and water molecules can diffuse through surface area, resulting in the rapid and complete shrinkage. For wide application of skin layer including utilizing it for pupal shell, eliminating this limit of dependency on composition is important.

1-1-3. Control of physical structure of polymer network

Thanks to the recent advance in the polymer synthesis technique, it became possible to control or enhance the functionalities of gels by controlling or newly designing the physical structure of polymer network rather than screening the monomer and polymer species. For example, Yoshida et al. prepared the comb-type grafted gel, which has thermoresponsive grafted polymers chemically

bonded to the thermoresponsive polymer network only at one terminal, and confirmed that this gel shows rapid shrinkage in response to temperature increase because grafted polymers have relatively high mobility and rapidly form hydrophobic aggregation cores inside the polymer network, which trigger the shrinkage of the surrounding network.[22]

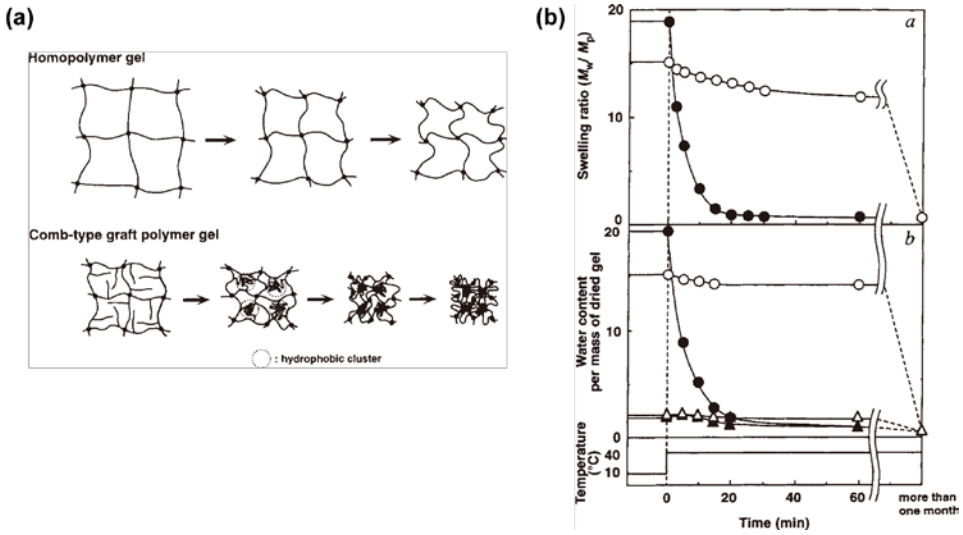

Figure 1-10. (a) Schematic image of the shrinking of comb-type grafted gel in comparison with conventional gel. (b) Time evolution of swelling ratio and water content of comb-type grafted gel and conventional one in response to temperature increase.[22]

Sakai et al. prepared the hydrogel which has very homogeneous polymer network by mixing two types of reactive group terminated four-arm poly(ethylene glycol) and crosslinking each other, so-called tetra-PEG gel.[23] Conventionally, the fragility of gels comes from the inhomogeneity of polymer network: stress concentrates short polymer strand and damage it. In the case of tetra-PEG gel, stress is distributed equally to whole polymer network, resulting in high physical

strength and good extension property.

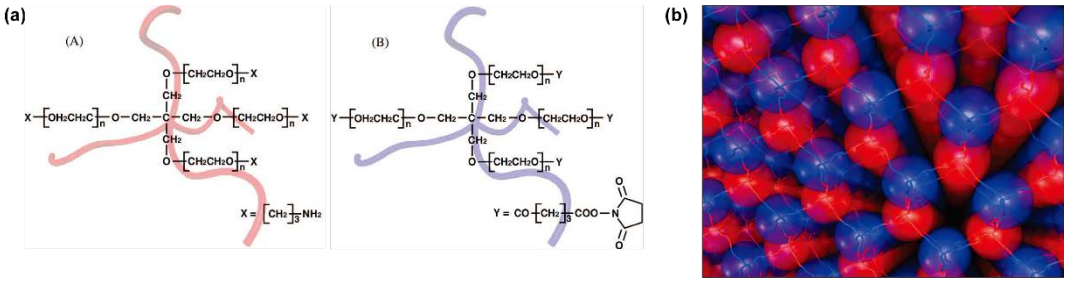

Figure 1-11. (a) Chemical structure of two types of reactive group terminated four-arm PEG as building blocks. (b) Schematic image of the polymer network of tetra-PEG gel.[23]

Furthermore, Okumura et al. successfully synthesized topological gel, which has end-capped PEG as a main chain and numeral eight-shaped cyclodextrin-derived crosslinker penetrated by main chains.[24] Main chain and crosslinker make polyrotaxane structure where they are not chemically bonded to each other and crosslinker can freely slide along main chain. This unique property enables effective relaxation of stress during stretching, resulting in high physical strength and good extension property like tetra-PEG gel.

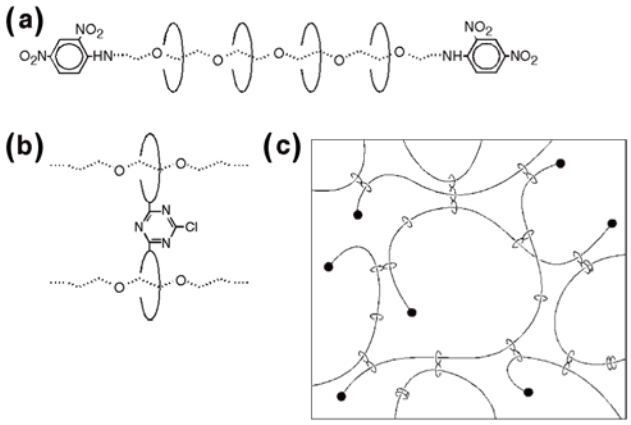

Figure 1-12. Schematic images of (a) polyrotaxane structure, (b) 8-shaped crosslinker, and (c) polymer network of topological gel.[24]

These novel functions obtained by precisely designing the physical structure of polymer network are essentially independent on the species of monomers and polymers. Therefore, it is expected that optimum design of polymer network can leads to the formation of skin layer independent on composition.

1-2. Scope of this research

The grand goal of this research is the creation of artificial larval state and metamorphosis. As the first step, this research aims the creation of reversible closed system utilizing skin layer of hydrogel, which will behave as a pupal shell. Here, I focused on the design of comb-type grafted gels. By introducing thermoresponsive grafted polymers only in the surface region of thermoresponsive hydrogel, which will induce the fast shrinkage of surface network, it is expected that the formation of dense skin layer in response to some external stimuli is promoted. The illustration is shown in Figure 1-13, and I call

the gels with this physical design of polymer network as “surface-grafted gels.”

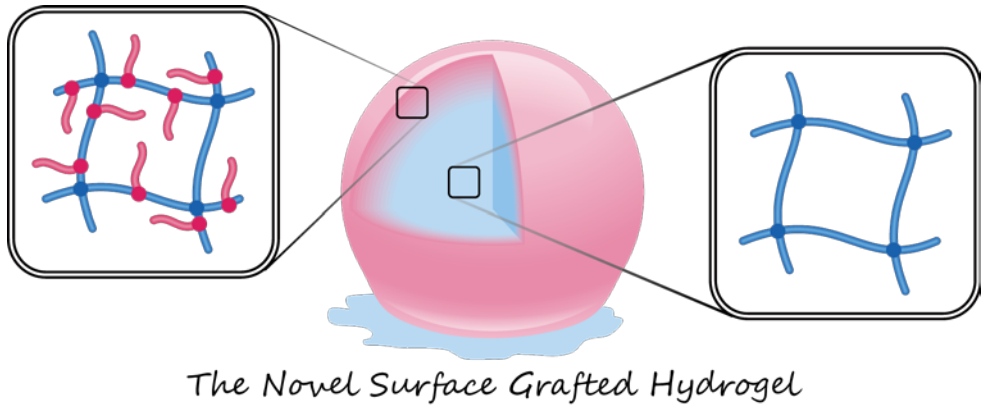

Figure 1-13. Illustration of surface-grafted hydrogels. Blue and red lines represent the base crosslinked polymer network and surface-grafted polymers, respectively.

In Chapter 2, a synthetic strategy of surface-grafted hydrogels is investigated. As a method of grafting polymer from the surface of hydrogels, activator regenerated by electron transfer for atom transfer radical polymerization (ARGET ATRP) was focused on. First, as a base material, hydrogels which is composed of the copolymer of *N*-isopropylacrylamide (NIPAAm) and *N*-(3-aminopropyl)methacrylamide (NAPMAm) were synthesized by free radical polymerization. Then, ATRP initiator with active ester group was reacted with the hydrogels with keeping them in shrunken state in poor solvent to introduce the initiator only in the surface region of the gels. Finally, ARGET ATRP of PNIPAAm was conducted from the introduced initiators to obtained thermoresponsive surface-grafted gels. The volume phase transition behavior of surface-grafted gels was mainly investigated in comparison with pristine

poly(NIPAAm-*r*-NAPMAm) gels using swelling equation.

In Chapter 3, thermoresponsive surface-grafted gels with various graft density were prepared by reacting ATRP initiator and structural analogous non-initiator to base gels simultaneously at the introduction step. First, the effects of graft density on the static properties such as micro- and macro-structure and Young's modulus of the surface are investigated. Then, the volume phase transition behavior was analyzed in relation with graft density and these static physical properties.

In Chapter 4, to explore the possibility of the control of the permeability through the surface of the gels only by the conformational change of surface-grafted polymers, the surface-grafted hydrogels which is composed of hydrophilic (non-thermoresponsive) polymer network and thermoresponsive surface-grafted polymers were prepared. Then, the swelling behavior from dried state to equilibrium swollen state at several temperatures are investigated to discuss the effect of temperature on the diffusion of water molecules from the outside to the inside through the surface of the gels.

Finally, in Chapter 5, the researched in this thesis are summarized, and future perspectives about the strategies to achieve the creation of "artificial pupa and metamorphosis" are described.

The researches about surface-grafted gels will give us the deep insight into the relation between "surface" and "bulk" of gels, which has not been vigorously studied before, and suggest the new strategy of physical design for the future studies on novel functional gels.

1-3. References

[1] Zhao, N.; Wang; Z.; Cai, C.; Shen, H.; Liang, F.; Wang, D.; Wang, C.; Zhu, T.; Guo, J.; Wang, Y.; Liu, X.; Duan, C.; Wang, H.; Mao, Y.; Jia, X.; Dong, H.; Zhang, X.; Xu, J. Bioinspired Materials: from Low to High Dimensional Structure. *Adv. Mater.* **2015**, *26*, 6994-7017.

[2] Heo, J.; Kang, T.; Jang, S. G.; Hwang, D. S.; Spruell, J. M.; Killops, K. L.; Waite, J. H.; Hawker, C. J. Improved Performance of Protected Catecholic Polysiloxanes for Bioinspired Wet Adhesion to Surface Oxides. *J. Am. Chem. Soc.* **2012**, *134*, 20139-20145.

[3] Izumi, H.; Suzuki, M.; Aoyagi, S.; Kanzaki, T. Realistic imitation of mosquito's proboscis: Electrochemically etched sharp and jagged needles and their cooperative inserting motion. *Sensor. Actuat. A* **2011**, *165*, 115-123.

[4] Guo, Z.; Zhou, F.; Hao, J.; Liu, W. Stable Biomimetic Super-Hydrophobic Engineering Materials. *J. Am. Chem. Soc.* **2005**, *127*, 15670-15671.

[5] Kondo, S.; Asai, R. A reaction-diffusion wave on the skin of the marine angelfish *Pomacanthus*. *Nature* **1995**, *376*, 765-768.

[6] Sagués, F.; Epstein, I. R. Nonlinear chemical dynamics. *Dalton Trans.* **2003**, *0*, 1201-1217.

[7] Yoshida, R.; Takahashi, T.; Yamaguchi, T.; Ichijo, H. Self-Oscillating Gel. *J. Am. Chem. Soc.* **1996**, *118*, 5134-5135.

[8] Ueki, T.; Yoshida, R. Recent aspects of self-oscillating polymeric materials: designing self-oscillating polymers coupled with supramolecular chemistry and ionic liquid science. *Phys. Chem. Chem. Phys.* **2014**, *16*, 10388-10397.

[9] Maeda, S.; Hara, Y.; Sakai, T.; Yoshida, R.; Hashimoto, S. Self-Walking Gel.

Adv. Mater. **2007**, *19*, 3480-3484.

[10] Murase, Y.; Maeda, S.; Hashimoto, S.; Yoshida, R. Design of a Mass Transport Surface Utilizing Peristaltic Motion of a Self-Oscillating Gel. *Langmuir* **2009**, *25*, 483-489.

[11] Shiraki, Y.; Yoshida, R. Autonomous Intestine-Like Motion of Tubular Self-Oscillating Gel. *Angew. Chem. Int. Ed.* **2012**, *51*, 6112-6116.

[12] Lowe, T.; Garwood, R. J.; Simonsen, T. J.; Bradley, R. S.; Withers, P. J. Metamorphosis revealed: time-lapse three-dimensional imaging inside a living chrysalis. *J. R. Soc. Interface* **2013**, *10*, 20130304.

[13] Tanaka, T. Collapse of Gels and the Critical Endpoint. *Phys. Rev. Lett.* **1978**, *40*, 820-823.

[14] Jeong, B.; Gutowska, A. Lessons from nature: stimuliresponsive polymers and their biomedical applications. *Trends Biotechnol.* **2002**, *20*, 305-311.

[15] Klouda, L.; Mikos, A. G. Thermoresponsive hydrogels in biomedical applications. *Eur. J. Pharm. Biopharm.* **2008**, *68*, 34-45.

[16] Liu, F.; Urban, M. W. Recent advances and challenges in designing stimuli-responsive polymers. *Prog. Polym. Sci.* **2010**, *35*, 3-23.

[17] Hu, J.; Liu, S. Responsive Polymers for Detection and Sensing Applications: Current Status and Future Developments. *Macromolecules* **2010**, *43*, 8315–8330.

[18] Ward, M. A.; Georgiou, T. K. Thermoresponsive Polymers for Biomedical Applications. *Polymers* **2011**, *3*, 1215-1242.

[19] Qiu, Y.; Park, K. Environment-sensitive hydrogels for drug delivery. *Adv. Drug. Deliver. Rev.* **2012**, *64*, 49–60.

[20] Matsuo, E. S.; Tanaka, T. Patterns in shrinking gels. *Nature* **1992**, *358*, 482-485.

[21] Matsumoto, A.; Ishii, T.; Nishida, J.; Matsumoto, H.; Kataoka, K.; Miyahara, Y. A Synthetic Approach Toward a Self-Regulated Insulin Delivery System. *Angew. Chem.* **2012**, *124*, 2166-2170.

[22] Yoshida, R.; Uchida, K.; Kaneko, Y.; Sakai, K.; Kikuchi, A.; Sakurai, Y.; Okano, T. Comb-type grafted hydrogels with rapid de-swelling response to temperature changes. *Nature* **1995**, *374*, 240-242.

[23] Sakai, T.; Matsunaga, T.; Yamamoto, Y.; Ito, C.; Yoshida, R.; Suzuki, S.; Sasaki, N.; Shibayama, M.; Chung, U. Design and fabrication of a high-strength hydrogel with ideally homogeneous network structure from tetrahedron-like macromonomers. *Macromolecules* **2008**, *41*, 5379-5384.

[24] Okumura, Y.; Ito, K. The Polyrotaxane Gel: A Topological Gel by Figure-of-Eight Cross-links. *Adv. Mater.* **2001**, *13*, 485-487.

Chapter 2:
Development of the Thermoresponsive Surface-Grafted Hydrogel by ARGET ATRP

2-1. Introduction

Recently, polymer surface-modification techniques have been advanced by the development of living radical polymerization (LRP). Atom-transfer radical-polymerization (ATRP) is a class of LRP and is widely used for the preparation of well-defined polymer grafted surfaces on solid substrates.[1] Furthermore, activator regenerated by electron transfer for ATRP (ARGET ATRP) has been developed to overcome the problems and limitations of ATRP such as sensitivity to oxygen and the need for a high copper catalyst concentration.[2] Simakova *et al.* succeeded in the controlled synthesis of poly(oligo(ethylene oxide) methyl ether methacrylate) in an aqueous media with a very low concentration of Cu catalyst,[3] and Matyjaszewski *et al*. reported the preparation of well-defined and highly dense polymer brushes on silicon wafers without the need for special equipment or deoxygenation using a surface-initiated ARGET ATRP method.[4] Because ARGET ATRP can proceed in water without need for solvent deoxygenation and with a low Cu concentration, it is a powerful tool for the surface-modification of water-based materials, including hydrogels.

In this chapter, I prepared a novel surface-grafted gel that has polymer chains grafted in a localized surface region of a bulk hydrogel by surface-initiated ARGET ATRP. ATRP initiators can be introduced locally in the surface region by introducing the initiator and carrying out the reaction in a poor solvent because a gel shrinks in a poor solvent and penetration of initiators into a gel network is suppressed.[5] For the first trial to create a surface-grafted gel, I selected the thermo-responsive polymer poly(*N*-isopropylacrylamide) (PNIPAAm), which is widely used in various biomedical applications,[6],[7] for the main and the grafted

chains of the gel. The thermoresponsive kinetics of the prepared gel was compared with that of a conventional non-grafted PNIPAAm gel.

2-2. Experimental

2-2-1. Materials

N-Isopropylacrylamide (NIPAAm) was kindly provided by KJ Chemicals (Tokyo, Japan) and purified by recrystallization in toluene/hexane. *N*-(3-Aminopropyl)methacrylamide (NAPMAm) was purchased from Polyscience (Warrington, PA) and used as received. *N*,*N*′-methylenebisacrylamide (MBAAm) was purchased from Acros Organics (Geel, Belgium) and used as received. Ammonium persulfate (APS) was purchased from Kanto Chemical (Tokyo, Japan). 8-Anilino-1-naphthalenesulfonic acid (ANS) and tris[2-(dimethylamino)ethyl]amine (Me_6TREN) were purchased from Tokyo Chemical Industry (Tokyo, Japan). *N*,*N*,*N*′,*N*′-tetramethylethylenediamine (TEMED), ethyl 2-bromoisobutyrate (EBiB), copper(II) bromide ($CuBr_2$), dehydrated dimethyl sulfoxide (DMSO), and dehydrated *N*,*N*-dimethylformamide (DMF) were purchase from Wako Pure Chemical Industries (Osaka, Japan). Water used in this study was purified by a water purifier (WA200, Yamato Scientific, Tokyo, Japan). 2-Bromoisobutanoic acid *N*-hydroxysuccinimide ester (abbreviated as NHS-ATRP-initiator) and 5-acryloylfluorescein (abbreviated as FLAAm) were synthesized as reported.[8],[9] 0.2 M Phosphate buffer (pH 7.5) was prepared by mixing disodium hydrogenphosphate and sodium dihydrogenphosphate (purchased from Wako Pure Chemical Industries) in

aqueous solution. 40-μL glass capillaries (inner diameter = 1.02 mm) were purchased from Hirschmann Laborgeräte (Eberstadt, Germany).

2-2-2. Synthesis of the cylindrical poly(NIPAAm-*r*-NAPMAm) gel

NIPAAm (0.806 g), NAPMAm (0.0268 g), MBAAm (0.0347 g), and TEMED (11.2 μL) were dissolved in water (4.5 mL), and the solution was degassed by Ar bubbling and cooled to 0 °C. Then a solution of APS (0.0171 g) in water (500 μL) was added, and the pre-gel solution was loaded into 40-μL glass capillaries (ϕ = 1.02 mm). The loaded capillaries were laid at 4 °C for 8 h. After this time, the cylindrical poly(NIPAAm-*r*-NAPMAm) gels (length = 20–30 mm) were obtained. The gels were purified by dialysis in water for one week. The obtained pre-modified gels are referred to as NG as an abbreviation of "non-grafted."

2-2-3. Immobilization of the ATRP initiator on the surface of the poly(NIPAAm-*r*-NAPMAm) gel

Poly(NIPAAm-*r*-NAPMAm) gels were immersed in 0.2 M phosphate buffer (pH 7.5, 27 mL) and the solution was heated to 60 °C to make gels shrink. NHS-ATRP-initiator (0.790 g) dissolved in dimethylsulfoxide (3 mL) was then added, and the mixture was stirred for 15 min. Then, the gels were retrieved and purified by dialysis in water for one week.

2-2-4. Grafting of PNIPAAm to the surface of the poly(NIPAAm-*r*-NAPMAm) gel

Initiator-immobilized poly(NIPAAm-*r*-NAPMAm) gels were immersed in a solution of NIPAAm (0.679 g), Me_6TREN (160 μL), $CuBr_2$ (13.4 mg), ascorbic acid (52.9 mg), and H_2O (30 mL), and the mixture was stirred for 3 h at 25 °C. Then, the gels were retrieved and purified by dialysis in water for one week. The obtained poly(NIPAAm-*r*-NAPMAm) gels with surface-grafted PNIPAAm are referred to as SG as an abbreviation of "surface-grafted."

Scheme 2-1. Synthesis of surface grafted gels: (1) the immobilization of the NHS-initiator to the surface of the gel, and (2) PNIPAAm grafting from the surface of the gel.

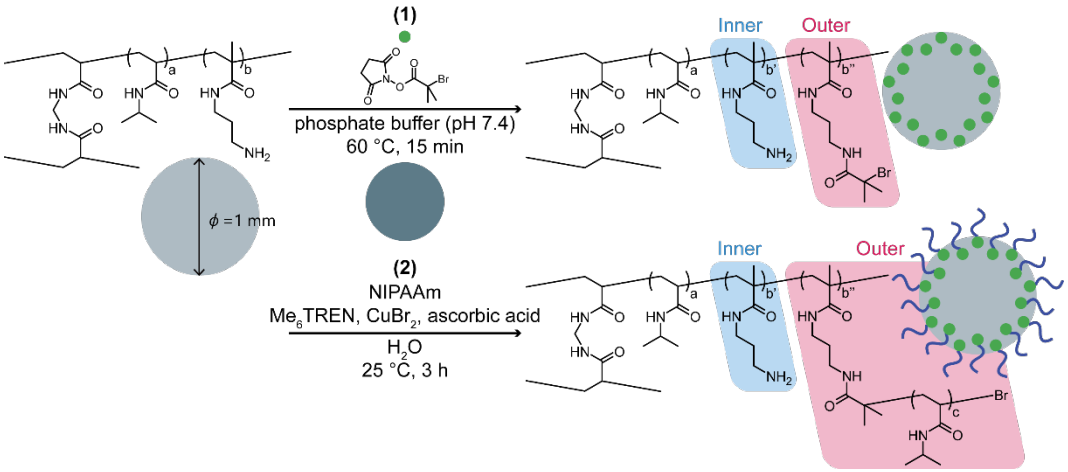

2-2-5. Differential scanning calorimetry of the surface-grafted gel

To measure the lower critical solution temperature (LCST) of the grafted polymer and the volume phase transition temperature (VPTT) of the polymer network, differential scanning calorimetry (DSC) was performed for both SG and NG under an N_2 gas atmosphere (using a DSC1, Mettler-Toledo, Tokyo, Japan). The temperature was raised from 10 to 60 °C at a heating rate of 10 °C/min. The cylindrical samples were cut into fragments of several milligrams weight. The

LCST and VPTT were defined by the peak tops of endothermic peaks.

2-2-6. Cross-sectional observation of the surface-grafted gel

To evaluate the spatial distribution of the surface-grafted polymers of the gels, FLAAm was copolymerized with NIPAAm by ARGET ATRP to graft fluorescent polymers to SG. Initiator-immobilized poly(NIPAAm-*co*-NAPMAm) gels were immersed in the mixture of NIPAAm (0.678 g), FLAAm (2.40 mg), Me_6TREN (160 μL), $CuBr_2$ (13.4 mg), ascorbic acid (52.9 mg), *N*,*N*-dimethylformamide (15 mL), and water (15 mL), and the mixture was stirred for 3 h at 0 °C. Then the gels were retrieved and purified by dialysis in DMF for 3 days, followed by dialysis in water for 4 days. The obtained gels were referred to as FSG. The cylindrical FSG was sliced into a disk shape (thickness < 1 mm) and placed on a glass plate with the flat area face-up. Then the sliced gel was observed by fluorescence microscopy (λ_{ex} = 494 nm, λ_{em} = 521 nm) (DFC 360FX, Leica, Mannheim, Germany).

2-2-7. Measurement of the equilibrium swelling ratio of the gels

NG and SG were immersed in water and maintained for 1 h at each temperature, ranging from 25 to 50 °C with 1 °C steps. Then the gels were observed by optical microscopy (VHX-900, Keyence, Osaka, Japan). The diameters of the gels on the pictures were measured using the Image J software (National Institute of Health, Bethesda, MD). Swelling ratios were calculated by dividing the diameter of the gel by the inner diameter of the mold glass capillary. To visualize the hydration and dehydration of the polymer network, NG and SG

were immersed in aqueous solutions containing ANS (10 mg/L) overnight, and the gels were subsequently observed by fluorescence microscopy at 25 °C (below volume phase transition temperature (VPTT)) and 40 °C (above VPTT) in the dilute ANS solution (λ_{ex} = 388 nm, λ_{em} = 470 nm). Images were recorded after the gels were maintained for 10 min at each temperature.

2-2-8. Kinetic analyses of shrinking and swelling of the gels

For shrinkage analyses, NG and SG were immersed in water and laid at 25 °C overnight. Then, the gels were placed in hot water (40 °C), and volume changes were observed using an optical microscope. The diameters of the gels on the pictures were measured using Image J. Swelling analyses were done in the same way except for reversing the temperature and drying the gels before immersing them in water at 40 °C.

2-3. Results and discussion

2-3-1. Synthesis of the surface-grafted gel

Colorless, cylindrical surface-grafted gels (SG) were obtained after ARGET ATRP step. At equilibrium state at 25 °C, fine wrinkles were observed on the surface of the SG, while the surface of the NG was smooth (Figure 2-1). These wrinkles are attributed to a mismatch between the swelling ratio of the interior and the surface of the SG gel.

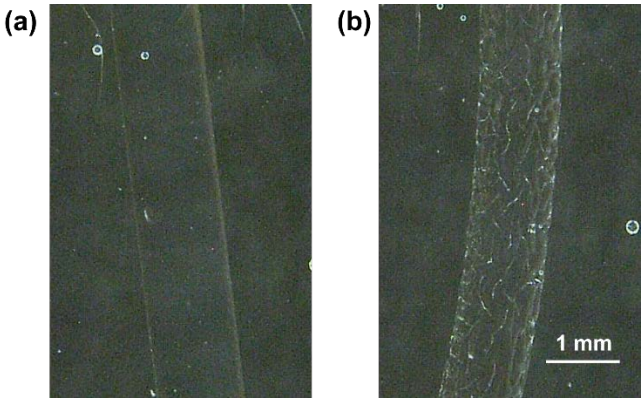

Figure 2-1. Photographs of (a) NG and (b) SG at 25 °C by optical microscope.

According to the result of DSC for SG and NG, SG had two endothermic peaks during heating; one at 33.7 °C deriving from the grafted PNIPAAm and one at 41.2 °C deriving from the poly(NIPAAm-*r*-NAPMAm) network, the former of which was not observed in the result of NG (Figure 2-2). This result indicates that the introduction of grafted polymer to the gels by ARGET ATRP successfully occurred, and the LCST of grafted polymer and the VPTT of polymer network were determined.

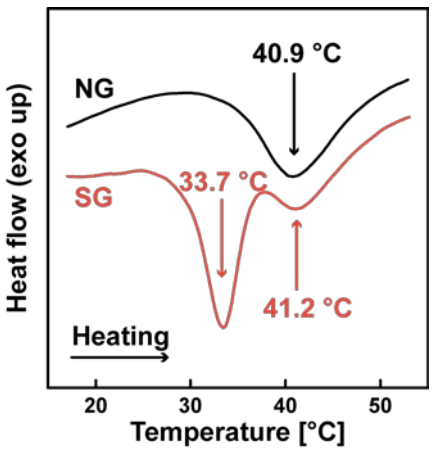

Figure 2-2. DSC thermograms of NG (black line) and SG (red line).

To estimate the molecular weight of the grafted polymer on the SG gel, free PNIPAAm was synthesized using free ATRP initiator (EBiB 22.3 μL) under the same synthetic conditions as that in the ARGET ATRP during the preparation of SG. Using gel permeation chromatography (GPC), the number average molecular weight and the polydispersity index (PDI) of the obtained free polymer were calculated as 8.3 kD and 2.0, respectively. The PDI was relatively high because of accelerated ARGET ATRP kinetics in aqueous solution.[10]

2-3-2. Evaluation of the spatial distribution of grafted polymer using fluorescent monomer

To evaluate the spatial distribution of grafted polymers in SG, a fluorescent monomer (FLAAm) was copolymerized grafted polymers (Figure 2-3(a)), and the cut face of the obtained gel (FSG) was observed by fluorescence microscopy (λ_{ex} = 494 nm, λ_{em} = 521 nm). As shown in Figure 2-3(b), fluorescence was observed from the cut face of the FSG gel, indicating that the grafted polymers were successfully introduced to the gel. Furthermore, the fluorescent intensity of the surface region (approximately with 200-μm thickness) was higher than that of the inside (Figure 2-3(c)), indicating that the grafted polymer was introduced with high density only in the surface region of the gel as expected because the diffusion of the NHS-ATRP-initiator in the gel was successfully suppressed during the initiator conjugation process.

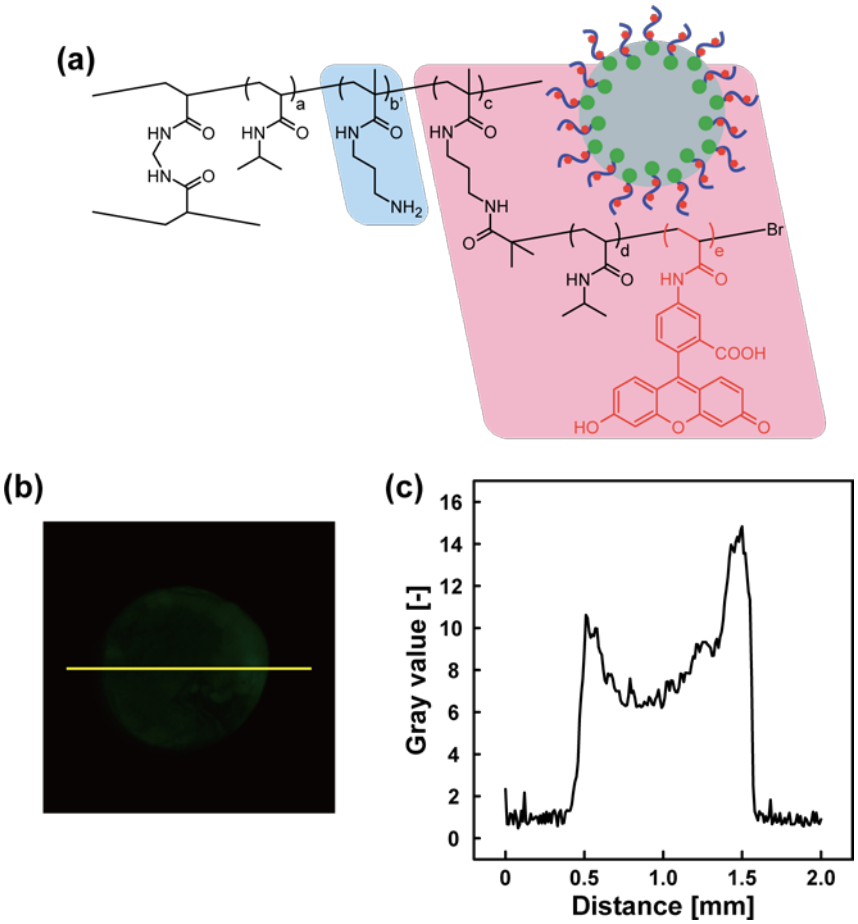

Figure 2-3. (a) Chemical structure of FSG. (b)Fluorescence image of cut face of sliced FSG. (c) The distribution of fluorescence intensity across the diameter of FSG (shown by the yellow line in (b)).

2-3-3. Equilibrium swelling ratio of the surface-grafted gel

To investigate the effect of thermoresponsive surface-grafted polymers on the thermoresponsive behavior of the gels, the equilibrium swelling ratios of NG and SG were measured in water at each temperature. Figure 2-4(a) shows the temperature dependence of the equilibrium swelling ratio of NG (black plots) and SG (red plots). NG, which is a conventional poly(NIPAAm-*co*-NAPMAm) gel, showed an LCST type volume phase transition behavior, with isotropic shrinkage

at temperatures higher than VPTT. In contrast, SG had a two-phase coexistence at temperatures around 40–45 °C, where both swollen and shrunken phases were observed simultaneously in the same gel (Figures 2-4(b) and 2-4(c)). This unique phase separation pattern is similar to the “bubble pattern” that can be observed during shrinking of acrylamide hydrogels on immersion in an acetone-water mixture, a poor solvent for acrylamide gels. In this phenomenon, the diffusion of solvent molecules through the surface is restricted due to the formation of a dense skin layer on the surface of the gel. Therefore, this result indicates that SG also formed a dense skin layer above VPTT. After the “bubble pattern” phase, the swollen area of SG suddenly cracked and started to shrink fast at around 45 °C. This result suggests that the dehydration and aggregation of the crosslinked polymer network proceeded during the two-phase coexistence, and the stress to polymer network gradually increased under constant volume condition. When this stress exceeded the mechanical strength of the polymer network, cracks formed. After the cracking, rapid shrinkage occurred due to exposure of the non-grafted, inside region of the gel.

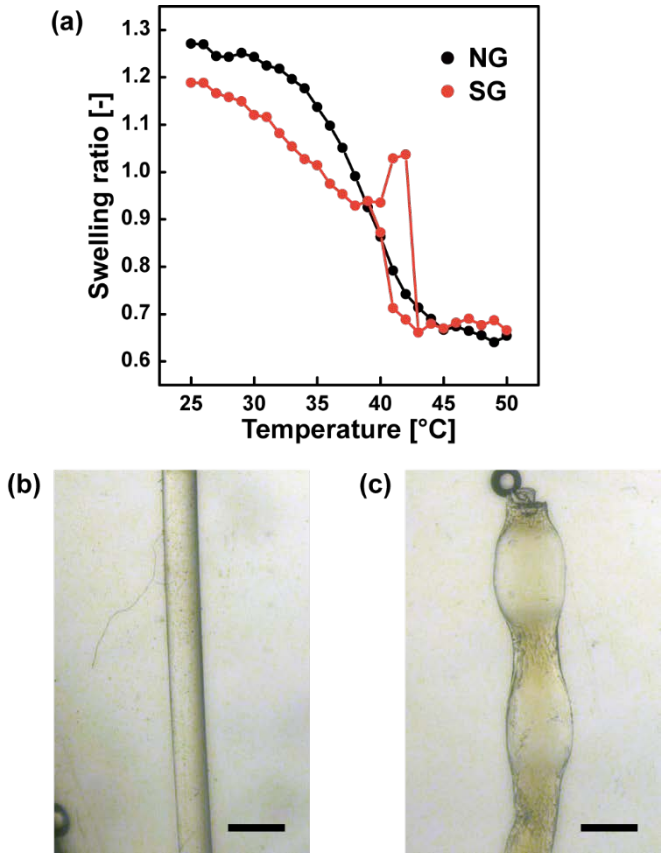

Figure 2-4. (a) Equilibrium swelling ratio of NG (black dots) and SG (red dots) over the studied temperature range. Photographs of (b) NG and (c) SG at around VPTT by optical microscope (black scale bar = 1 mm).

To analyze the shrinking behavior of the gels in more detail, NG and SG were immersed in an aqueous solution containing ANS (1 mg/L) and observed by fluorescence microscopy (λ_{ex} = 388 nm, λ_{em} = 470 nm). The fluorescence of ANS can only be observed with this wavelength when the surrounding environment is hydrophobic. Thus, hydration and dehydration of the polymer network can be visualized by fluorescence microscopy in ANS aqueous solution. Figure 2-5 shows the fluorescence microscopy images of NG and SG at 25 °C (below the VPTT) and at 50 °C (above the VPTT). Below the VPTT (25 °C),

both gels were in a swollen state and did not exhibit fluorescence. On the other hand, above the VPTT (50 °C), SG maintained its swollen state but fluoresced slightly, while NG shrank and fluoresced strongly from the whole gel. These results indicate that SG formed a dense skin layer with dehydration of the grafted polymer network and suppressed solvent molecule diffusion, while the NG gel did not form a skin layer because the polymer network of NG is highly hydrophilic due to the copolymerization with hydrophilic NAPMAm. Previous study showed that when thermoresponsive grafted polymers are introduced homogeneously to the whole thermoresponsive gel network (so-called comb-type grafted gels), rapid shrinkage occurs due to the hydrophobic interactions between rapidly dehydrated grafted polymer chains and crosslinked polymer main chains. In the case of the surface-grafted gels, it is expected that such a rapid shrinkage occurred only in surface polymer network and thus the formation of a dense skin layer was induced even with a particular composition of polymer network which does not originally form a skin layer.

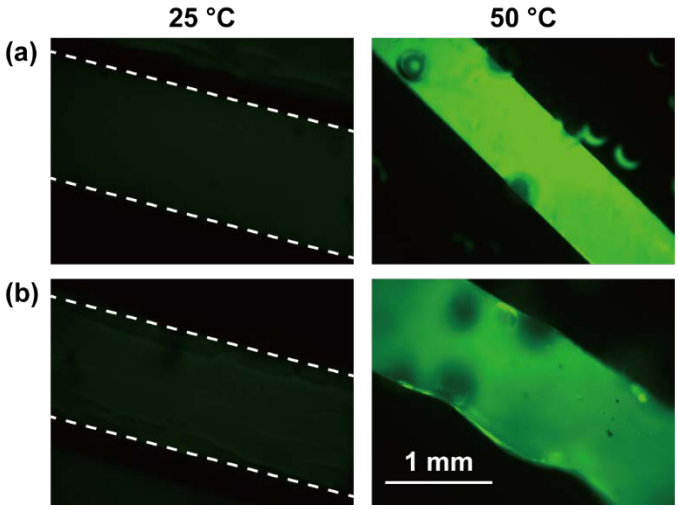

Figure 2-5. Fluorescence images by fluorescence microscope (λ_{ex} = 388 nm, λ_{em} = 470 nm) of (a) NG and (b) SG at 25 °C (left) and 50 °C (right) in 1 mg/L ANS aqueous solution. White broken lines represent the outlines of the gels.

2-3-4. Kinetics analysis of shrinkage and swelling of the surface-grafted gel

To evaluate the effect of the introduction of surface-grafted polymers on the kinetics of shrinking and swelling behavior of the thermoresponsive gels, a sudden temperature increase from 25 °C to 50 °C and decrease from 50 °C to 25 °C were applied to both NG and SG, and the time evolution of the swelling ratios was measured. Time evolution of swelling ratio during shrinkage is shown in Figure 2-6. NG rapidly shrank immediately after temperature increase, without the formation of a skin layer, and an almost totally shrunken state was obtained after 15 min. In contrast, SG maintained a swollen state for a defined period due to the formation of a dense skin layer. Furthermore, approximately 15 minutes after the temperature increase, a crack formed on the surface of the gel and it started to shrink rapidly. This crack occurred because the graft-polymer network of the gel was not able to sustain the tension generated by the crosslinked

polymer network inside the gel; this is the same phenomenon observed in the equilibrium swelling measurements.

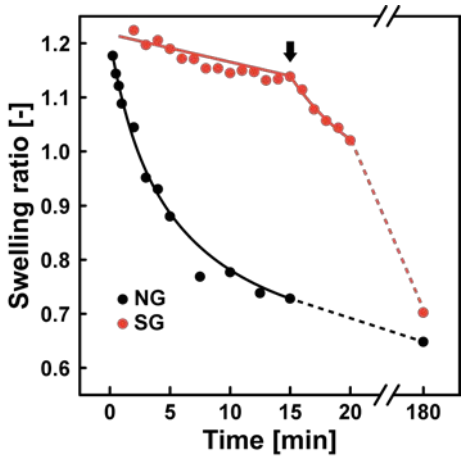

Figure 2-6. The change in swelling ratio of NG (black dots) and SG (red dots) with time during shrinking process induced by a temperature increase (25 → 50 °C). Black arrow represents the timing of cracking of SG.

The time evolution of the swelling ratio during the swelling process is shown in Figure 2-7. From these plots, d_n is calculated with Equation (2-1) and shown in the insets. d_∞ and d_0 are the swelling ratio in the equilibrium state and at time zero, respectively.

$$d_n = \frac{d_\infty - d(t)}{d_\infty - d_0} \tag{2-1}$$

The relationship between the relaxation time (τ) and the cooperative diffusion coefficient (D) for a cylindrical gel can be written as follows.

$$D = \frac{3{d_\infty}^2}{8\pi^2\tau} \tag{2-2}$$

D can also be described by the elastic modulus of the polymer network (K) and the friction between the polymer network and the solvent molecules (f), as shown

in Equation (2-3).

$$D = \frac{K}{f} \tag{2-3}$$

In the case of NG, a relaxation mode with τ = 32 min was observed. On the other hand, SG showed slower swelling with τ = 45 min than that of NG. Slow relaxation might be attributed to large friction between the dense polymer network in the surface region and the solvent molecules which diffused though the surface region into the gel; the large *f* results in small *D* by Equation (2-2).

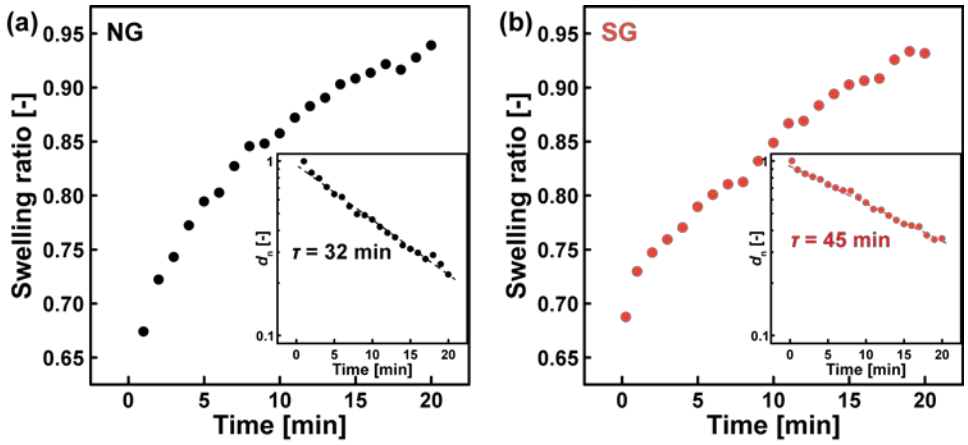

Figure 2-7. Change in the swelling ratio of (a) NG and (b) SG with time during the swelling process induced by a temperature increase (50 → 25 °C). Insets in each graph: Plots of d_n against time, and the relaxation time calculated from the slope of the straight line.

2-4. Conclusion

Surface-grafted hydrogels were successfully synthesized by immobilization of the ATRP initiator to the surface region of the gels and a subsequent ARGET ATRP step. Fluorescence microscopy revealed that the grafted polymers were

successfully introduced to the gel surface region using a fluorescent comonomer as a probe of the grafted polymers. In equilibrium swelling ratio measurement, a two-phase coexistence called bubble pattern was observed, suggesting the formation of a dense skin layer at the surface of the gel. Fluorescence microscopy in dilute ANS aqueous solution also indicated the formation of skin layer. This is expected to be because the grafted polymer induced fast shrinkage of the polymer network in the surface region in the same way as the fast shrinking of comb-type grafted gels. During the shrinkage induced by temperature increase, surface-grafted gels maintained a swollen state for a defined time with the formation of a dense skin layer, and then shrank rapidly with cracking because the inner stress exceeded the mechanical strength of the dehydrated polymer network and the interior non-grafted network was exposed. As for the swelling process, surface-grafted gels showed a slower relaxation than pristine gels. This might be attributed by the large friction between the highly dense surface polymer network and solvent molecules diffusing through surface into gels. To our best knowledge, this is the first example of a bulk hydrogel with a dense surface-localized layer of grafted polymers and an “active” permeation control of the gels. From the view point of creating artificial pupal shell, this design strategy has a great potential to overcome the problem of the dependency of the skin layer formation on the composition of polymer network.

2-5. References

[1] Matyjaszewski, K. Atom transfer radical polymerization (ATRP): Current

status and future perspectives. *Macromolecules* **2012**, *45*, 4015-4039.

[2] Jakubowski, W.; Matyjaszewski, K. Activators regenerated by electron transfer for atom transfer radical polymerization of styrene. *Macromolecules* **2006**, *39*, 39-45.

[3] Simakova, A.; Averick, S. E.; Konkolewicz, D.; Matyjaszewski, K. Aqueous ARGET ATRP. *Macromolecules* **2012**, *45*, 6371-6379.

[4] Matyjaszewski, K.; Dong, H.; Jakubowski, W.; Pietrasik, J.; Kusumo, A. Grafting from surfaces for “everyone”: ARGET ATRP in the presence of air. *Langmuir* **2007**, *23*, 4528-4531.

[5] Mizutani, A.; Nagase, K.; Kikuchi, A.; Kanazawa, H.; Akiyama, Y.; Kobayashi, J.; Annaka, M.; Okano, T. Effective separation of peptides using highly dense thermo-responsive polymer brush-grafted porous polystyrene beads. *J. Chromatogr. B* **2010**, *878*, 2191-2198.

[6] Nagase, K.; Kobayashi, J.; Kikuchi, A.; Akiyama, Y.; Kanazawa, H.; Okano, T. Effects of graft densities and chain lengths on separation of bioactive compounds by nanolayered thermoresponsive polymer brush surfaces. *Langmuir* **2008**, *24*, 511-517.

[7] Hiruta, Y.; Shimamura, M.; Matsuura, M.; Maekawa, Y.; Funatsu, T.; Suzuki, Y.; Ayano, E.; Okano, T.; Kanazawa, H. Temperature-responsive fluorescence polymer probes with accurate thermally controlled cellular uptakes. *ACS Macro Lett.* **2014**, *3*, 281-285.

[8] Conradi, M.; Junkers, T. Fast and efficient [2 + 2] UV cycloaddition for polymer modification via flow synthesis. *Macromolecules* **2014**, *47*, 5578-5585.

[9] Serpe, M. J.; Jones, C. D.; Lyon, L. A. Layer-by-layer deposition of thermoresponsive microgel thin films. *Langmuir* **2003**, *19*, 8759-8764.

[10] Brounecker, W. A.; Tsarevsky, N. V.; Gennaro, A.; Matyjaszewski, K. Thermodynamic components of the atom transfer radical polymerization equilibrium: Quantifying solvent effects. *Macromolecules* **2009**, *42*, 6348-6360.

Chapter 3:
Investigation of Effect of Graft Density on Physical Properties of Surface-Grafted Gels

3-1. Introduction

In the synthesis of the surface-grafted gels, grafted polymers are introduced by ARGET ATRP. It enables introduction of well-defined grafted polymers in an aqueous solution without degassing and with low amounts of copper catalysts, and easy control of various polymerization parameters, including the monomer species, molecular weight, and graft density[1]-[3]. Among them, the parameter of graft density is quite important because it could determine the total amount of the grafted polymer, morphologies of the surface, and degree of exposure of base materials. For polymer-grafted solid substrates, such as glass and silica, there have been many studies about the effect of the graft densities. For example, Yoshikawa *et al.* prepared poly(2-hydroxyethyl methacrylate)-grafted surfaces on silicon wafers with different graft densities using a grafting-from or grafting-to method, and revealed that the adsorption of aprotinin to polymer-grafted surfaces is strongly dependent on the graft densities[4]. Feng *et al.* also prepared poly(2-methacryloloxyethyl phosphorylcholine)-grafted surfaces with different graft densities by introducing polymerization initiators and initiator analogs (non-initiators) at a certain ratio, and succeeded in controlling the roughness and wettability of the surface[5]. In addition, Nagase *et al.* prepared poly(*N*-isopropylacrylamide)-grafted silica beads and confirmed that the graft density controlled the interaction with steroid molecules[6].

For my thermoresponsive surface-grafted gels, it is still unclear how the graft density of the surface-grafted polymer affects the bulk properties of the gels. Herein, surface-grafted gels with different graft densities were prepared by

simultaneously introducing an ATRP initiator and structurally analogous non-initiator to the surface of the gels. Then, I discuss their effects on the bulk properties of the surface-grafted gels represented by their shrinking and swelling behaviors.

3-2. Experimental

3-2-1. Materials

N-Isopropylacrylamide (NIPAAm) was kindly provided by KJ Chemicals (Tokyo, Japan) and purified by recrystallization in toluene/hexane. *N*-(3-Aminopropyl)methacrylamide (NAPMAm) was purchased from PolyScience (Warrington, PA) and used as received. *N*,*N*'-methylenebisacrylamide (MBAAm) was purchased from Acros Organics (Geel, Belgium) and used as received. Ammonium persulfate (APS) was purchased from Kanto Chemical (Tokyo, Japan). Tris[2-(dimethylamino)ethyl]amine (Me_6TREN) was purchased from Tokyo Chemical Industry (Tokyo, Japan). *N*,*N*,*N*',*N*'-tetramethylenediamine (TEMED), *N*-succinimidyl acetate (abbreviated as NHS-non-initiator), $CuBr_2$, pyridine, and dehydrated dimethyl sulfoxide (DMSO) were purchase from Wako Pure Chemical Industries (Osaka, Japan). The water used in this study was purified using a water purifier (Elix Essential 3 (UV), Merck Millipore, Billerica, MA, USA). 2-Bromoisobutanoic acid *N*-hydroxysuccinimide ester (abbreviated as NHS-ATRP-initiator) was synthesized as previously reported[7]. A glass

capillary (40 μL, inner diameter = 1.02 mm) was purchased from Hirschmann Laborgeräte (Eberstadt, Germany).

3-2-2. Synthesis of the cylindrical/disk-shaped poly(NIPAAm-*r*-NAPMAm) gel

NIPAAm (0.806 g, 95 mol%), NAPMAm (0.0268 g, 2 mol%), MBAAm (0.0347 g, 3 mol%), and TEMED (11.2 μL) were dissolved in water (4.5 mL), and the solution was degassed by Ar bubbling and cooled to 0 °C in ice bath. Then, a solution of APS (0.0171 g) in water (500 μL) was added, and the pre-gel solution was placed into 40-μL glass capillaries (inner diameter = 1.02 mm) or between two glass slides with a silicone sheet spacer (thickness = 1 mm). The loaded capillary and glass mold were maintained at 4 °C for 8 h. After that, the cylindrical poly(NIPAAm-*r*-NAPMAm) gel (length = 20–30 mm) and sheet gel were obtained. The sheet gel was cut into a disk shape (diameter = 2.1 mm). The gels were purified by dialysis in water for one week. The obtained pre-modified gels are referred to as NG. They were dried in air at 25 °C for 1 day prior to the next step.

3-2-3. Immobilization of the ATRP initiator in the surface region of the poly(NIPAAm-*r*-NAPMAm) gel

A water (28 mL) and pyridine (1 mL) mixture was heated to 60 °C. Then, naturally-dried pre-modified gels and NHS-ATRP-initiator/NHS-non-initiator (see Table 3-1) dissolved in DMSO (1 mL) were added, and the mixture was stirred for 5 min. It had been confirmed that this reaction using poor solvent condition for

the PNIPAAm derivative gels enables the introduction of ATRP initiator only in the surface region of the gels as mentioned in Chapter 2. The gels were purified by dialysis in water for one week. The obtained gels are hereafter referred to as SG*x*, where *x* denotes the feed molar ratio (%) of the NHS-ATRP-initiator.

Table 3-1. The amounts of NHS-ATRP-initiator and NHS-non-initiator used for the immobilization reaction of the ATRP initiator.

Sample	NHS-ATRP-initiator [g] (molar ratio [%])	NHS-non-initiator [g] (molar ratio [%])
SG100	0.079 (100)	0 (0)
SG50	0.040 (50)	0.024 (50)
SG25	0.020 (25)	0.035 (75)

3-2-4. Grafting of PNIPAAm from the surface region of the poly(NIPAAm-*r*-NAPMAm) gel

Initiator-immobilized poly(NIPAAm-*r*-NAPMAm) gels were immersed in a solution of NIPAAm (0.679 g), Me_6TREN (160 μL), $CuBr_2$ (13.4 mg), ascorbic acid (52.9 mg), and H_2O (30 mL), and the mixture was stirred for 3 h at 25 °C. Then, the gels were purified by dialysis in water for one week. The whole synthetic scheme is shown in Scheme 3-1. The dry masses of the samples were measured after drying them in air at 25 °C for 1 day. Since the increment in the dry mass corresponds to the total amount of grafted polymers, the dry masses can be converted to graft densities, σ, by Equation 3-1:

$$\sigma\ [\mu g/mm^2] = \frac{\Delta m}{\pi \cdot 1.05\ [mm]^2 \cdot 2 + 2\pi \cdot 1.05\ [mm] \cdot 1\ [mm]} \quad (3\text{-}1)$$

where Δm represents the increment in dry mass.

Scheme 3-1. Schemes for (1) the immobilization of NHS-ATRP-initiator and NHS-non-initiator to the surface of the gels and (2) PNIPAAm grafting from the surface of the gels.

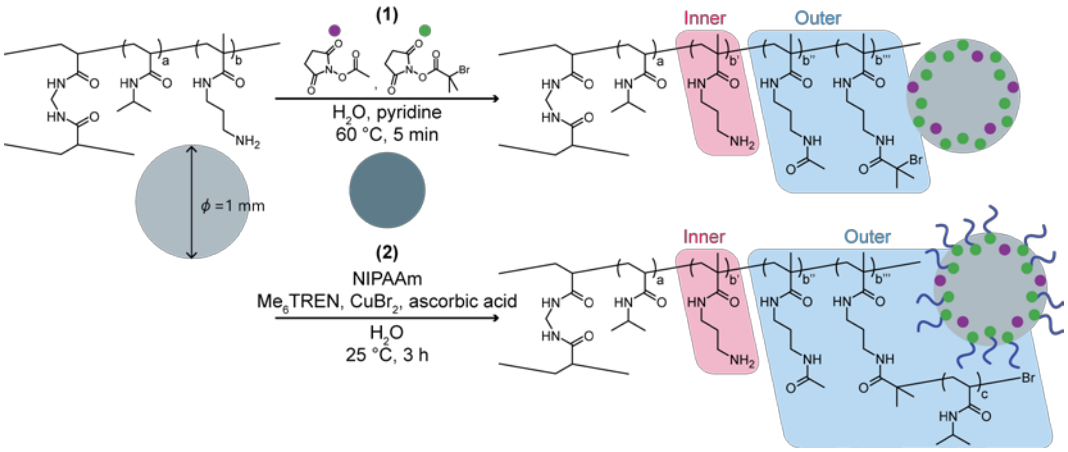

3-2-5. Measurement of the total amount of bromine introduced to the surface-grafted gels

The total amount of Br atoms derived from the ATRP initiator that chemically bonded to the polymer network of the gels was measured by elemental analysis. Disk-shaped "pre-grafted" SG100, which does not contain a grafted polymer but has an immobilized ATRP initiator, was pre-treated using an AQF-2100H high temperature hydropyrolysis system (Mitsubishi Chemical Analytech, Kanagawa, Japan) and analyzed by ion chromatography (ICS-1600, Dionex, Sunnyvale, CA, USA).

3-2-6. Observation of the surface macroscopic profile of the disk-shaped gels

The surface profiles (roughness) of NG and the surface-grafted gels were observed using 3D measuring laser microscopy (OLS4100, Olympus, Tokyo, Japan) in water at 25 °C. The observed area was 485×485 μm^2.

3-2-7. Measurement of the Young's moduli of the disk-shaped gels

The Young's moduli of the surface of NG and the surface-grafted gels were measured using atomic force microscopy (AFM; Flex-AFM, Nanosurf, Liestal, Switzerland) using force curve measurements in water at 25 °C (cantilever: MikroMasch OPUS 240AC-GG, spring constant: 1.24 N/m, set point: 10 nN, recording distance: 1 μm, deflection sensitivity: 151 nm/V). The obtained force curves were fitted to Fung's model using the AtomicJ software[8]. The measurement was conducted three times for each sample.

3-2-8. Observation of the surface polymer networks of the gels

The surface polymer networks of NG and SG100 were observed using cryo-scanning electron microscopy (SEM; Hitachi SU8200, cryo system: Quorum Cryosystem PP3010T, 1.0-kV acceleration voltage, -140 °C stage temperature, ×10.000 magnification).

3-2-9. Kinetic analyses of the shrinking and swelling of the NG and SG gels

For the shrinking analyses, the disk-shaped NG and the surface-grafted gels were firstly dried in air at 25 °C for 1 day, and then immersed in water and kept at 30 °C overnight. Then, the gels were placed in hot water at 45 °C and the weight was measured each hour using a balance. For the swelling analyses, cylindrical gels were kept in hot water at 50 °C overnight, and the time evolution of the volume was observed by optical microscopy in cool water (25 °C). The diameters of these gels were measured using the ImageJ software (National Institute of Health, Bethesda, MD). Temperatures were selected based on the

LCST of PNIPAAm grafted on SG100, 34 °C, and VPTT of NG, 41 °C, which is mentioned in Chapter 2, and the smaller step size, compared with that for swelling analyses, was selected for shrinking analyses to avoid the crack formation on the surface of the gels.

3-3. Results and discussion

3-3-1. Synthesis of the surface-grafted gels with various graft densities

All samples are colorless transparent gels in equilibrium states at 25 °C. As shown in Table 2, the dry mass increases in proportion to the molar ratios of the introduced ATRP initiator and structurally analogous non-initiator (Table 3-2). Moreover, the graft density is successfully controlled by reacting the initiator and non-initiator simultaneously to the surface of the gel at a certain ratio, as shown in Figure 3-1. Thus, I could successfully synthesize surface-grafted gels with various graft densities.

Table 3-2. The dry mass of one disk of each sample and its increment compared with that of NG.

Sample	Dry mass [mg]	Increment [mg]
SG100	1.35	0.20
SG50	1.28	0.13
SG25	1.22	0.07
NG	1.15	-

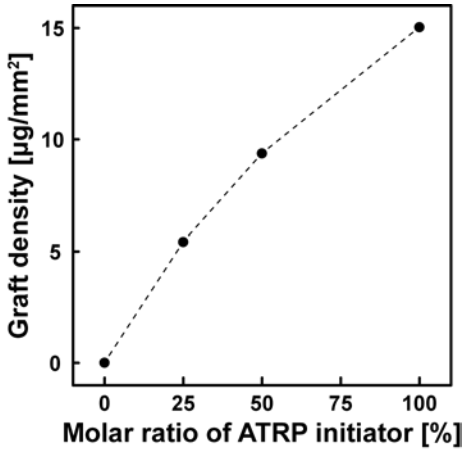

Figure 3-1. The dependence of the graft density on the molar ratio of the NHS-ATRP-initiator / NHS-non-initiator.

In addition, the elemental analysis revealed that "pre-grafted" SG100 contains 860 μg/g of Br, which is derived from the ATRP initiator. Supposing that ARGET ATRP proceeds homogeneously from all bromine atoms, the number-average molecular weight of the grafted polymer could be estimated as 1.4×10^4 g/mol by dividing the increment in dry mass by the total amount of Br atom.

Some of the surface-grafted gels have fine wrinkles on their surfaces. 3D measuring laser microscopy reveals that SG100 and SG50 have fine surface wrinkle patterns of 20 μm in depth and 100 μm in pitch, and 15 μm in depth and 70 μm in pitch, respectively, while the surfaces of SG25 and NG are flat (Figure 3-2). Such a wrinkle pattern is formed by a mismatch between the swelling ratios of the inner and outer regions of the gels[9]. In this case, the local osmotic pressure increases by post-modification of the grafted polymer to the surface region of the polymer network, and the surface region re-swells to relax the local

network. To measure the Young's modulus of the surface region of the gels, AFM force curve measurements were conducted. The obtained force curves correspond with the theoretical curve of Fung's model, and the Young's modulus calculated from the fitting curve is lower at higher graft densities (Figure 3-3), which indicates a large re-swelling. If the Young's modulus of the inner region of the surface-grafted gel is comparable to that of the surface of NG, this result indicates that the surface-grafted gels with higher graft densities have larger mismatches between the swelling ratios of the inner (non-grafted) and outer (grafted) regions of the gels, which is attributed to the increased osmotic pressure and results in the formation of particular wrinkle patterns.

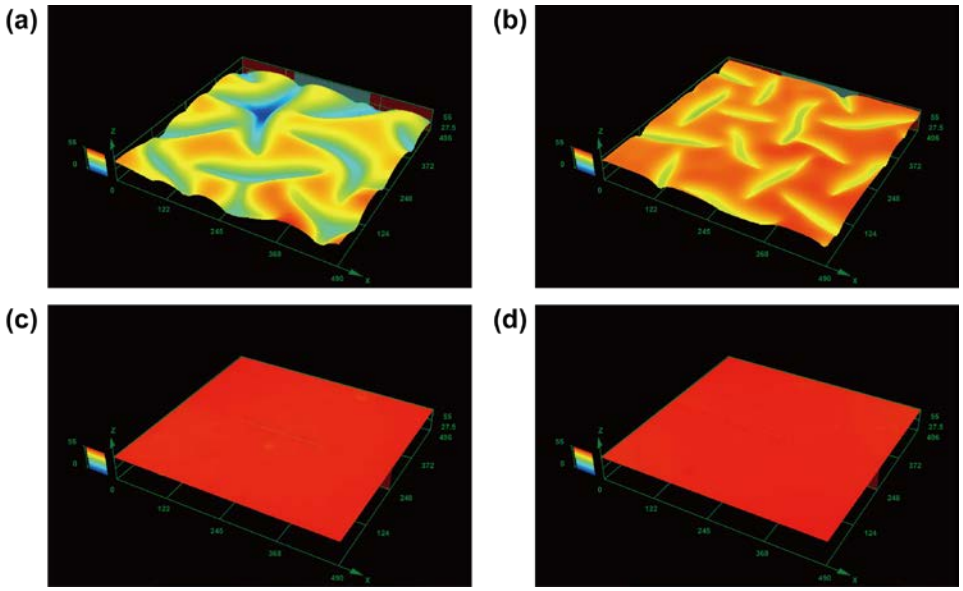

Figure 3-2. 3D measuring laser microscopy images of the surface of (a) SG100, (b) SG50, (c) SG25, and (d) NG. The square size is 485×485 μm^2.

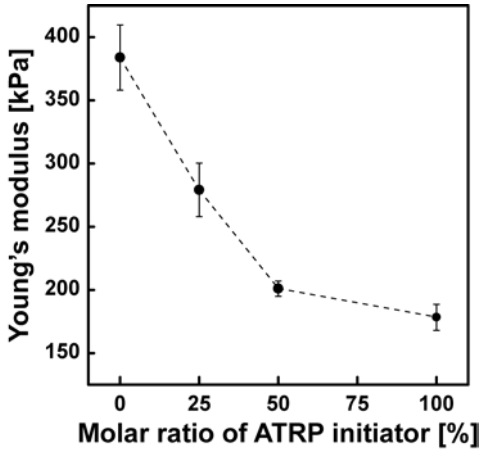

Figure 3-3. The dependence of the Young's modulus of the surfaces of the gels on the molar ratio of the NHS-ATRP-initiator/NHS-non-initiator. Data expressed are the means of triplicate measurements.

Furthermore, to evaluate the difference between the physical structures of the swollen polymer networks in the outer region of the pre-modified gel and the surface-grafted gels, cryo-SEM observations were conducted for NG and SG100, as representative samples. The obtained images reveal that the polymer network of SG100 has smaller pores and a more homogeneous structure than NG (Figure 3-4). This result is caused by the post-modification of the grafted polymers, which fill up the large pores of the inhomogeneous polymer network, enhancing the apparent homogeneity of the gel surface.

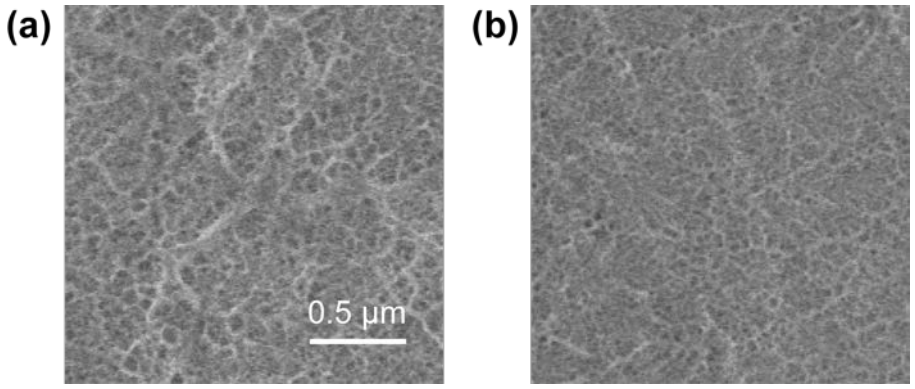

Figure 3-4. Cryo-SEM images of the surface polymer network in the outer region of (a) NG and (b) SG100.

3-3-2. Analyses of the shrinking process

To analyze the kinetics of the shrinking behavior in response to heating, a stepwise temperature increase from 30 °C to 45 °C was applied to NG and the surface-grafted gels, and the time evolution of the normalized weight was observed. As shown in Figure 3-5, NG begins to shrink immediately after the temperature increase and reaches the equilibrium shrunken state within approximately 1 h. However, the surface-grafted gels shrink slowly with the formation of skin layers. I confirmed that the shrinking speed decreases with increasing graft density. A previous report about gel-containing grafted polymers in its entire polymer network (so-called comb-type grafted gels) revealed that the grafted polymer that was introduced to the polymer network, which had a higher mobility than the crosslinked network polymer, could quickly form hydrophobic cores; the cores attracted a peripheral polymer network, resulting in the fast shrinkage of the entire gel[10]. In this study, grafted polymers were introduced only to the surface of the gels; therefore, such a fast shrinkage occurs only at the surface, and it induces the formation of skin layers. In

addition, the introduction of grafted polymers increases the polymer density of the surface region. As the polymer density is strongly correlated to the water permeability of the skin layer, the shrinking speed could also be controlled by changing the graft density.

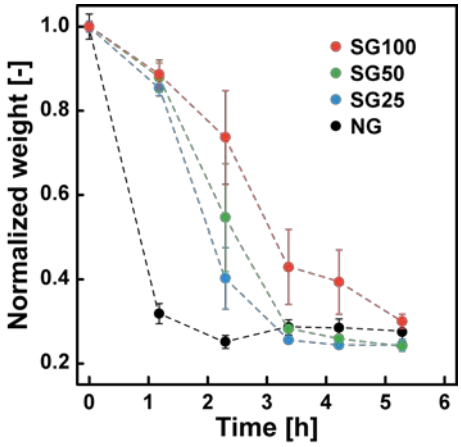

Figure 3-5. Time evolution of the normalized weight of SG100 (red), SG50 (green), SG25 (blue), and NG (black), and response to the temperature increase from 30 to 45 °C. The weight of the gel was normalized by the weight of each sample at 30 °C. Data expressed are the means of triplicate measurements.

3-3-3. Analyses of the swelling processes

Next, to analyze the swelling behavior in response to cooling, a stepwise temperature decrease from 50 °C to 25 °C was applied to the samples, and the time evolution of the swelling ratio was observed by optical microscopy. As shown in Figure 3-6(a), all the samples swelled in a monotonous manner after the temperature change. From these plots, the cooperative diffusion constant, *D*, was calculated by Equation 3-2 and 3-3[11]:

$$d_n = \frac{d_\infty - d(t)}{d_\infty - d_0} \propto e^{-\frac{t}{\tau}} \quad (3\text{-}2)$$

$$D = \frac{3{d_\infty}^2}{8\pi^2\tau} = \frac{K}{f} \quad (3\text{-}3)$$

where d_∞, d_0 and $d(t)$ represent the normalized swelling ratio of equilibrium state, initial state, and each time when observed, and K and f represent the bulk modulus of the polymer network and the friction constant between polymer network and solvent molecules, respectively. In this case, the volume fraction of outer region is relatively small, so the cooperative diffusion constant was calculated based on the hypothesis that the relaxation of swelling can be expressed with only one relaxation time. The calculations show that the surface-grafted gel with a higher graft density has a smaller cooperative diffusion constant (i.e., slower swelling) (Figure 3-6(b)). The reason D decreases after polymer grafting is mainly attributed to the increase in f. Although D is determined by f and K as shown in Equation 3-3, I consider that the effect of f, which is governed by the surface character, might be larger than that of K, which is governed by the bulk character, because the permeation of water molecules through the surface of a gel must be a rate-controlling step for the diffusion process. The increase in f after polymer grafting can be confirmed by the cryo-SEM images of NG and SG100, shown in Figure 3-4. The introduction of a grafted polymer enhances the homogeneity of the polymer network, where it is known that the increase in homogeneity of the polymer network decreases in its permeability, i.e., increases f.[12]

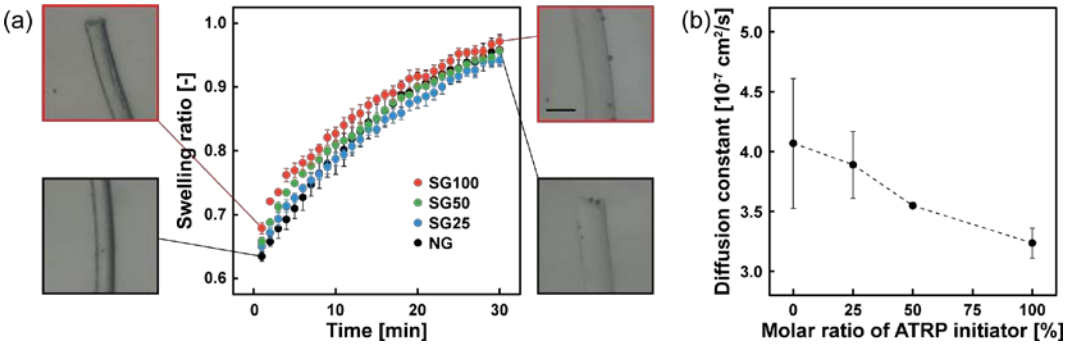

Figure 3-6. (a) Time evolution of the swelling ratios normalized by the diameter of the gels of SG100 (red), SG50 (green), SG25 (blue), and NG (black) in response to the temperature decrease from 50 to 25 °C, and the appearances of SG100 and SG25 at 30 sec and 30 min (scale bar in the picture: 1 mm). (b) The dependence of the relaxation time of the swelling behavior on the ratio of the NHS-ATRP-initiator / NHS-non-initiator. Data expressed are the means of triplicate measurements.

3-4. Conclusion

Poly(NIPAAm-*r*-NAPMAm) gels with only grafted PNIPAAm in the surface region with various graft densities were successfully synthesized by simultaneously introducing ATRP initiators and non-initiators at certain ratios while keeping the gels in a shrunken state; subsequent ARGET ATRP of PNIPAAm was performed in aqueous media. By measuring the dry mass of the surface-grafted gels and pre-modified gels, the graft density could be controlled by the ratio of ATRP initiators and non-initiators. 3D measuring laser microscopy in water revealed that the SGs had a specific wrinkle pattern on their surfaces, and their depths and pitches depended on the graft density. The Young's modulus and the polymer network homogeneity were both controlled by the graft density, which were confirmed by AFM force curve measurements and

cryo-SEM observations, respectively. These static properties, which were controlled by the graft density, directly affected the dynamic properties of the gels. During the shrinking process in response to the temperature increase, the surface-grafted gels formed dense skin layers, and their permeabilities were lower with higher graft densities, resulting in slower shrinkage. During the swelling process in response to the temperature decrease, SGs with higher graft densities had smaller cooperative diffusion constants (i.e., slower swelling). These results suggest that the static and dynamic properties of hydrogels can be precisely controlled by tuning the graft density of their surfaces, which means that the characteristics of gels as “open” or “semi-closed” systems are now arbitrarily controllable using this surface-localized polymer grafting method.

3-5. References

[1] Braunecker, W. A.; Matyjaszewski, K. Controlled/living radical polymerization: Features, developments, and perspectives. *Prog. Polym. Sci.* **2007**, *32*, 93–146.

[2] Pintauer, T.; Matyjaszewski, K. Atom transfer radical addition and polymerization reactions catalyzed by ppm amounts of copper complexes. *Chem. Soc. Rev.* **2008**, *37*, 1087–1097.

[3] Matyjaszewski, K.; Dong, H.; Jakubowski, W.; Pietrasik, J.; Kusumo, A. Grafting from Surfaces for “Everyone”: ARGET ATRP in the Presence of Air. *Langmuir* **2007,** *23,* 4528-4531.

[4] Yoshikawa, C.; Goto, A.; Tsujii, Y.; Fukuda, T.; Kimura, T.; Yamamoto, K.; Kishida, A. Protein Repellency of Well-Defined, Concentrated Poly(2-hydroxyethyl methacrylate) Brushes by the Size-Exclusion Effect. *Macromolecules* **2006,** *39,* 2284-2290.

[5] Feng, W.; Brash, J. L.; Zhu, S. Non-biofouling materials prepared by atom transfer radical polymerization grafting of 2-methacryloloxyethyl phosphorylcholine: Separate effects of graft density and chain length on protein repulsion. *Biomaterials* **2006**, *27*, 847–855.

[6] Nagase, K.; Kobayashi, J.; Kikuchi, A.; Akiyama, Y.; Kanazawa, H.; Okano, T. Effects of Graft Densities and Chain Lengths on Separation of Bioactive Compounds by Nanolayered Thermoresponsive Polymer Brush Surfaces. *Langmuir* **2008,** *24,* 511-517.

[7] Conradi, M.; Junkers, T. Fast and efficient [2 + 2] UV cycloaddition for polymer modification via flow synthesis. *Macromolecules* **2014**, *47*, 5578-5585.

[8] Hermanowicz, P.; Sarna, M.; Burda, K.; Gabryś H. AtomicJ: An open source software for analysis of force curves. *Rev. Sci. Instrum.* **2014**, *85*, 063703.

[9] Arifuzzaman, M.; Wu, Z. L.; Kurosawa, T.; Kakugo, A.; Gong, J. P. Swelling-induced long-range ordered structure formation in polyelectrolyte hydrogel. *Soft Matter*, **2012**, *8*, 8060-8066.

[10] Yoshida, R.; Uchida, K.; Kaneko, Y.; Sakai, K.; Kikuchi, A.; Sakurai, Y.; Okano, T. Comb-type grafted hydrogels with rapid de-swelling response to temperature changes. *Nature* **1995**, *374*, 240-242.

[11] Shibayama, M.; Nagai K. Shrinking kinetics of poly(*N*-isopropylacrylamide) gels *T*-jumped across their volume phase transition temperatures. *Macromolecules* **1999**, *32*, 7461-7468.

[12] Tokita, M.; Tanaka T. Reversible decrease of gel-solvent friction. *Science* **1991**, *253*, 1121-1123.

Chapter 4:

Control of Physical Properties of Gels Only by Conformational Change of Surface-Grafted Polymers

4-1. Introduction

It is possible to control the permeability of polymer membrane by introduction of grafted polymers inside the membrane and conformational change of the polymers. Maeda *et al.* synthesized a polymer which is composed of poly(butyl methacrylate) backbone and poly(*β*-benzyl L-aspartate) branch, and prepared a film with microdomains of poly(aspartic acid) by hydrolyzation.[1] When the film is immersed in aqueous solution at pH 9, poly(aspartic acid) forms random coil structure and sodium ions and water molecules can diffuse through the microdomains. Then, when the film is immersed in solution at pH 3, conformation of poly(aspartic acid) changes to *α*-helix, and the transport rate of Na^+ significantly decreased. This dependency can be explained by "through polymer" mechanism; the collapse of grafted polymers increases the polymer density and lowers the permeability as a result. On the other hand, the porous membrane of tetrafluoroethylene / ethylene copolymer with 10-μm pores with grafted poly(*γ*-benzyl L-glutamate), which was reported by Ito *et al.*,[2] shows an opposite controllability. Immersion of the membrane in solution at low pH induces the conformational change of grafted poly(glutamic acid) to *α*-helix and the increase in permeability, and immersion at high pH induces the change of the grafted polymer to random coil and the decrease in permeability. This dependency can be explained by "through pore" mechanism this time; the collapse of grafted polymers enlarges the inner diameter of pores and recovers the permeability.

Up to this chapter, the permeability of the surface region of thermoresponsive hydrogels is controlled by the reversible formation of skin layer

induced by the aggregation of thermoresponsive grafted polymers. However, if the permeability can be controlled only by the conformational change of grafted polymers, polymer network does not need to be thermoresponsive, which means the enhancement of flexibility of polymer design. In this Chapter 4, to achieve this goal with through-polymer mechanism, the preparation of the surface-grafted gels which is composed of hydrophilic network and thermoresponsive grafted polymers, and the evaluation of the control of permeability in response to temperature change by the analysis of swelling behavior are reported.

4-2. Experimental

4-2-1. Materials

N-Isopropylacrylamide (NIPAAm) was kindly provided by KJ Chemicals (Tokyo, Japan) and purified by recrystallization in toluene/hexane. *N*-(3-Aminopropyl)methacrylamide (NAPMAm) was purchased from PolyScience (Warrington, PA) and used as received. *N,N*'-methylenebisacrylamide (MBAAm) was purchased from Acros Organics (Geel, Belgium) and used as received. Ammonium persulfate (APS) was purchased from Kanto Chemical (Tokyo, Japan). Tris[2-(dimethylamino)ethyl]amine (Me_6TREN) was purchased from Tokyo Chemical Industry (Tokyo, Japan). *N,N*-Dimethylacrylamide (DMAAm), $CuBr_2$, pyridine, and dehydrated dimethyl sulfoxide (DMSO) were purchase from Wako Pure Chemical Industries (Osaka, Japan). DMAAm was purified using alumina column to remove stabilizer. The water used in this study was purified using a

water purifier (Elix Essential 3 (UV), Merck Millipore, Billerica, MA, USA). 2-Bromoisobutanoic acid *N*-hydroxysuccinimide ester (abbreviated as NHS-ATRP-initiator) was synthesized as previously reported.

4-2-2. Synthesis of the disk-shaped poly(DMAAm-*r*-NAPMAm) gel

DMAAm (0.594 mL, 77 mol%), NAPMAm (0.2681 g, 20 mol%), MBAAm (0.0347 g, 3 mol%), and APS (0.0342 g) were dissolved in water (5 mL), and the solution was degassed by three-time freeze-pump-thaw technique. Then, the pre-gel solution was placed between two glass slides with a silicone sheet spacer (thickness = 1 mm). The loaded glass mold was maintained at 50 °C for 24 h. After that, the obtained sheet gel was cut into a disk shape (diameter = 3.5 mm). The gels were purified by dialysis in water for one week. The obtained pre-modified gels are referred to as NG.

4-2-3. Immobilization of the ATRP initiator in the surface region of the poly(DMAAm-*r*-NAPMAm) gel

The pre-modified gels were immersed in a solution of water (28 mL) and pyridine (1 mL). Then, NHS-ATRP-initiator (0.0792 g) dissolved in DMSO (1 mL) was added, and the mixture was stirred vigorously for 5 min. After that, the solution was removed and the gels were purified by dialysis in water for one week. The obtained gels are referred to as SG.

4-2-4. Grafting of PNIPAAm from the surface region of the poly(DMAAm-*r*-NAPMAm) gel

Initiator-immobilized poly(DMAAm-*r*-NAPMAm) gels were immersed in a solution of NIPAAm (0.170 g), Me_6TREN (160 μL), $CuBr_2$ (13.4 mg), ascorbic acid (52.9 mg), and H_2O (30 mL), and the mixture was stirred for 3 h at 25 °C. Then, the gels were purified by dialysis in water for one week. The whole synthetic scheme is shown in Scheme 4-1.

Scheme 4-1. Schemes for (1) the immobilization of NHS-ATRP-initiator to the surface of the poly(DMAAm-*r*-NAPMAm) gel and (2) the PNIPAAm grafting from the surface of the gel.

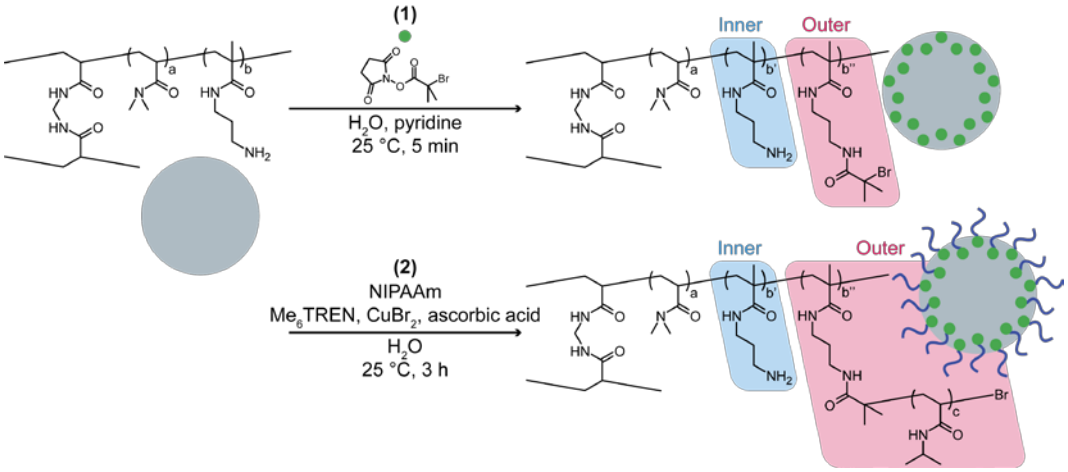

4-2-5. Kinetic analyses of the swelling behavior of NG and SG gels

NG and SG were firstly dried in air at 25 °C for 2 days. Then, the gels were placed in water at 20 °C or 50 °C, and the time evolution of the volume was observed by optical microscopy. The diameters of the gels were measured using the ImageJ software (National Institute of Health, Bethesda, MD). Volume was normalized into dimensionless swelling ratio by dividing the diameter of gels by the diameter of the gel as prepared (3.5 mm).

4-3. Results and discussion

4-3-1. Synthesis of the surface-grafted gels of hydrophilic network and thermoresponsive grafted polymers

Colorless, disk-shaped gels were obtained after ARGET ATRP step. At equilibrium state at 25 °C, fine wrinkles were observed on the surface of SG, while the surface of NG was smooth (Figure 4-1). The wrinkles seem to be owing to a mismatch between the swelling ratio of the inside and the surface region of SG, indicating the successful introduction of grafted polymers only in the surface region of the gels.

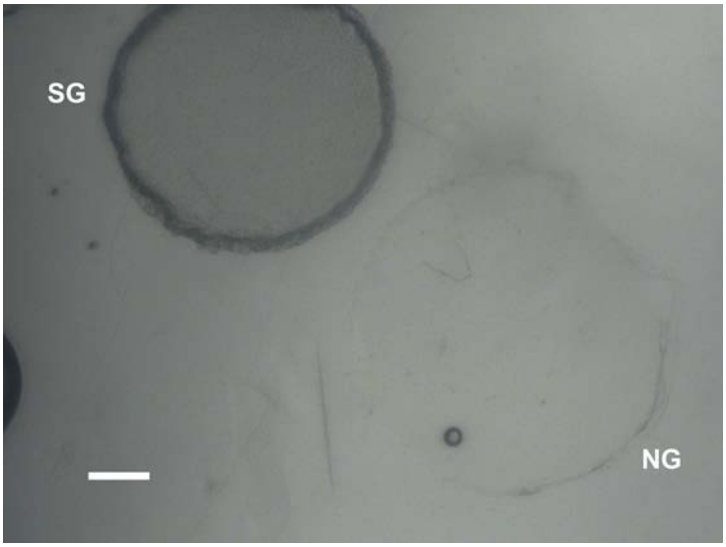

Figure 4-1. Photograph of NG (lower right) and SG (upper left) in equilibrium state at 25 °C by optical microscope. White scale bar = 1 mm.

4-3-2. Kinetic analyses of the swelling behavior of NG and SG gels

To evaluate the effect of the introduction of surface-grafted polymers and temperature on the diffusion of water molecules from the outside to the inside

through the surface region of the gels, naturally-dried gels were immersed in water at 25 °C or 50 °C, and the time evolution of the swelling ratio was measured. As shown in Figure 4-2(a) and (b), all the samples at both temperatures showed two-step relaxation, which is a typical swelling mode in the case-II transition. After the first relaxation, NG showed the fast and monotonous swelling, and almost reached equilibrium state within 15 min. In contrast, while SG showed the similar monotonous swelling at 25 °C, the volume change of SG at 50 °C was very small, almost constant. From these plots, the cooperative diffusion constant, *D*, was calculated by Equation 4-1 and 4-2:

$$d_n = \frac{d_\infty - d(t)}{d_\infty - d_0} \propto e^{-\frac{t}{\tau}} \tag{4-1}$$

$$D = \frac{3{d_\infty}^2}{8\pi^2\tau} = \frac{K}{f} \tag{4-2}$$

where d_∞, d_0 and $d(t)$ represent the normalized swelling ratio of equilibrium state, initial state, and each time when observed, and τ, K and f represent the relaxation time, the bulk modulus of the polymer network and the friction constant between polymer network and solvent molecules, respectively. In the case of NG, as shown in Figure 4-2(c), the diffusion constant at 50 °C is twice larger than that at 25 °C, which is owing to the increase in thermal mobility. Here, the relation between diffusion constant and temperature can be written by Stokes-Einstein equation:

$$D = \frac{kT}{6\pi\eta\xi} \tag{4-3}$$

where k, T, η, and ξ represent Boltzmann's constant, temperature, dynamic viscosity, and correlation length, respectively. This equation indicates that D is in proportion to T. However, the results of this study showed larger effect of T

on *D*. This difference may be caused by the analysis on too complex two-step swelling, and the discussion needs further investigation including measurements at other temperatures. In the case of SG, the value of diffusion constant is smaller than that of NG at both temperatures. This is attributed to the increase in homogeneity of polymer network in surface region by introduction of grafted polymers which causes the increase in *f* and the decrease in *D*. In addition, significant decrease in diffusion constant was observed at 50 °C compared with the value at 25 °C. The result suggests that the conformational change of grafted polymers from random coil to globule enhanced the polymer density of the surface region of SG, and this resulted in the increase in *f* and the decrease in *D*. It is also suggested that the effect of conformational change of grafted polymer on swelling behavior is much larger than that of the increase in thermal mobility.

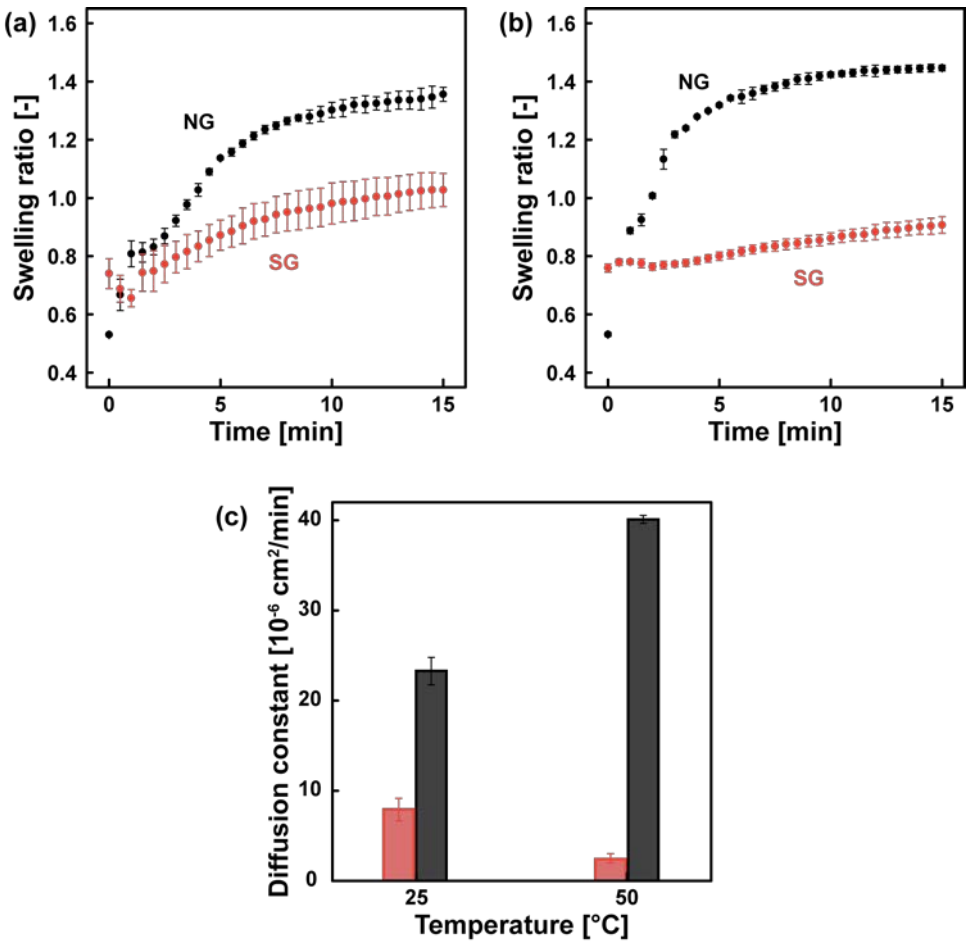

Figure 4-2. Time evolution of swelling ratio of NG (black dots) and SG (red dots) in water (a) at 25 °C and (b) at 50 °C, and (c) cooperative diffusion constant of NG (black bars) and SG (red bars) calculated from these plots.

4-4. Conclusion

Surface-grafted gels composed of poly(DMAAm-*r*-NAPMAm) network and surface-grafted PNIPAAm were successfully synthesized by reacting NHS-ATRP-initiator with poly(DMAAm-*r*-NAPMAm) gels for very short time to introduce initiators only in the surface region of gels and a subsequent ARGET ATRP of PNIPAAm from the initiators. They had fine wrinkle pattern on its

surface, which indicates the successful introduction of surface-grafted polymers. As for swelling behavior from dried state to equilibrium swollen state in water, pristine poly(DMAAm-*r*-NAPMAm) gels and surface-grafted gels showed case-II transition (two-step swelling). Pristine gels showed fast monotonous swelling in the second relaxation both at 25 °C and 50 °C, where the relaxation at 50 °C is faster than that at 25 °C due to the increase in thermal mobility. In contrast, surface-grafted gels showed very slow relaxation at 50 °C in comparison with that at 25 °C, which attributed the conformational change of PNIPAAm from random coil to globule. These results suggest that it is possible to control the permeability through the surface region of the gels only by the conformational change of surface-grafted polymers. I must admit that the control is not complete yet, and the diffusion from inside to outside through the surface of the gels also must be investigated by some methods. However, this design has a potential to achieve the goal: the creation of artificial pupal shell.

4-5. References

[1] Maeda, M.; Kimura, M.; Hareyama, Y.; Inoue, S. pH-Dependent Ion Transport across Polymer Membrane, pH-Induced Reversible Conformational Change of Transmembrane Poly(L-aspartic acid) Domain in Polymer Membrane. *J. Am. Chem. Soc.* **1984**, *106*, 251-253.

[2] Ito, Y.; Ochiai, Y.; Park, Y. S.; Imanishi, Y. pH-Sensitive Gating by Conformational Change of a Polypeptide Brush Grafted onto a Porous Polymer Membrane. *J. Am. Chem. Soc.* **1997**, *119*, 1619-1623.

Chapter 5:

Conclusion

5-1. Summary

In this research, the novel functional hydrogel whose only surface polymer network is precisely designed was created. Recently, biomimetic or bioinspired materials are vigorously researched to realize the superior functions which animals and plants have. Most of the functions have not only spatial but also temporal orders derived from dissipative structure in non-equilibrium open system. Especially, metamorphosis is very attractive from the view point of biomimetic and bioinspired materials because this phenomenon has long time-scale, from days to years, and functions significantly change through it. However, this attractive phenomenon has not been targeted in this field. To achieve "artificial metamorphosis," the pupal state, which is peculiar to complete metamorphosis, is focused on, and this research first aims the creation of pupal shell utilizing skin layer. In more detail, to utilize skin layer with arbitrary polymer composition, the surface-grafted gel which has grafted polymers only in the surface region of the gel is designed based on the idea of comb-type polymer network which enables fast shrinkage of network.

In Chapter 2, thermoresponsive surface-grafted gels were successfully synthesized by immobilization of ATRP initiators only in the surface region of the gels and subsequent ARGET ATRP of grafted polymers. The VPTT of base polymer network and the LCST of grafted polymers was 41 °C and 34 °C, respectively. Fine wrinkle pattern on the surface was observed in equilibrium swollen state due to the mismatch between the swelling ratio of inside and outside of the gels. The surface-grafted gels also exhibit unique shrinking pattern called "bubble pattern" around volume phase transition temperature. In addition,

during shrinking process in response to temperature increase, the period of constant volume was observed. As for swelling behavior, the speed of swelling is affected by this design, i.e., the speed is lowered. These results indicate that the formation of skin layer was successfully induced by the introduction of surface-grafted polymers, and the bulk properties are critically dominated the physical design of surface network.

In Chapter 3, the graft density of surface-grafted gels was controlled by reacting ATRP initiators and structurally analogous non-initiators at a certain ratio simultaneously to the gels. The pattern of wrinkles on their surface was correlated to graft density. The enhancement of homogeneity of surface polymer network was confirmed caused by the introduction of grafted polymers. Young's modulus of the surface was lower with higher graft density. These static properties affected the dynamic volume change properties. The permeability of skin layer during shrining process decreased and the speed of swelling also decreased as the graft density increased. It was revealed that the graft density is a critical parameter for the properties of surface-grafted gels, and the properties are now arbitrarily controllable.

In Chapter 4, the surface-grafted gels which is composed of hydrophilic polymer network and thermoresponsive surface-grafted polymers were successfully synthesized. The fine wrinkle patterns were also observed on their surface. Though the gels did not show the volume phase transition in response to temperature change, the speed of swelling from dried state to equilibrium swollen state was much lower at high temperature above the LCST of grafted polymers than at low temperature below LCST. From these results, it is

suggested that the control of permeability of the surface of gels is possible only by the conformational change of grafted polymers rather than the formation of skin layer.

In summary, functional hydrogels which have novel physical structure of polymer network called surface-grafted hydrogels have been created. Note that the surface-grafted gels have unique properties which conventional hydrogels do not have; i.e., (1) only the surface network is precisely designed, (2) a dense skin layer can be formed in response to temperature change, and (3) the permeability of the surface can be arbitrarily controlled with arbitrary composition of polymer network. The essences of this research can be described as follows; (a) the focus on the surface of gels of bulk size, (b) the design methods and strategies for synthesis of gels, and (c) discussion about the relationship between static “surface” properties and dynamic “bulk” properties of gels.

5-2. Future perspectives

The grand goal of this study is the creation of artificial pupa and metamorphosis. In this chapter, future perspectives to reach the goal are mainly focused on. As mentioned in previous chapters, this study succeeded in the reversible control of hydrogels between open system and semi-closed system using the design of surface-grafting. Why I used the term “semi-”closed here is that since the base polymer network in Chapter 2 and 3 has thermoresponsiveness, the state where the volume of the gels is constant with skin layer formation is not equilibrium state but steady state. In addition, in Chapter 4, the complete

suppression of mass diffusion through the surface only by grafted polymers is not achieved yet. The next steps to be achieved for the grand goal that (i) the achievement of the reversible "complete" closed system by hydrogels, (ii) the utilization of the inside of the gels of closed or semi-closed system as a field of chemical reaction, and (iii) the design of polymer network which exhibits the significant change in functions comparable to that from juvenile to adult form in metamorphosis. I explain them one by one below.

First, as for the step (i). Since skin layer and aggregation layer of grafted polymers still have a certain level of water content, it is difficult to completely suppress the diffusion of water molecules and substrates soluble in water through the layers. This problem will be solved by coating the gels surface with ionic liquids (ILs). ILs are the molten salts composed only of cations and anions, and their melting point is below room temperature. Up to now, many unique properties as solvent such as thermal and chemical stability, non-volatility, incombustibility have been reported.[1] In addition, some ILs including 1-ethyl-3-methylimidazolium bis(trifluoromethylsulfonyl)imide ($[C_2mim][NTf_2]$) are known to be hydrophobic and dissolve PNIPAAm with upper critical solution temperature (UCST).[2] Focusing on these properties, the coating of the surface of surface-grafted gels with these ILs will be investigated by immersing the gels which are composed of hydrophilic polymer network and surface-grafted PNIPAAm in ILs at higher temperature than LCST of PNIPAAm which causes dehydration and IL-solvation of PNIPAAm. This method enables to effectively suppress the diffusion of water molecules and substrates insoluble in the ILs without losing elasticity. Furthermore, thanks to the hydrophobicity and

non-volatility of ILs, achievement of “non-dryable” hydrogels is also expected, which will promote much wider applications of hydrogels.

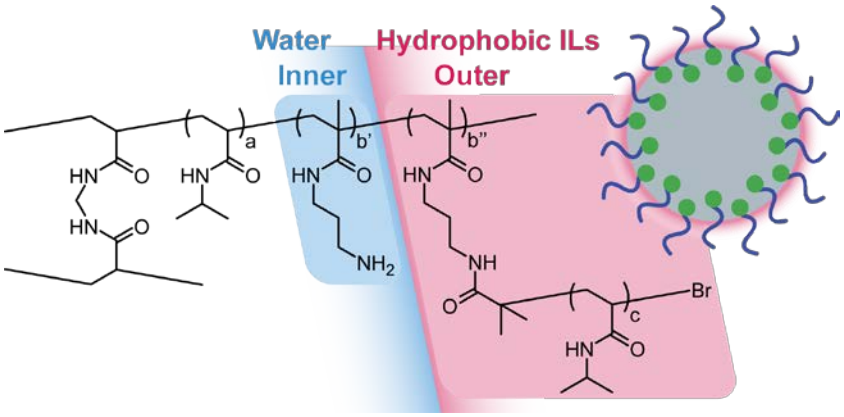

Figure 5-1. Schematic image of the non-dryable gel which is composed hydrophilic PDMAAm network and surface-grafted PNIPAAm, and coated with hydrophobic ILs.

Second, as for the step (ii) the utilization of the inside of the gels of closed or semi-closed system as a field of chemical reaction, the application for self-oscillating gels will be investigated. As mentioned in Chapter 1, self-oscillating gels should be immersed in BZ substrates solution during volume oscillation. However, by applying the design of surface-grafting and controlling open system and closed system, it is expected to achieve smarter self-oscillating gels which completely incorporate BZ reaction inside. This system can neglect the contamination of outer solution by BZ substrates (acids and oxidants), and the inhibition of BZ reaction by outer substrates such as chlorides. In addition, since the formation of skin layer induces unique shrinking patterns, there is a possibility to observe the volume oscillation in different oscillating mode from the

conventional one.

Finally, as for the step (iii) the design of polymer network which exhibits the significant change in functions comparable to that from juvenile to adult form in metamorphosis, I suggest the novel functional gel which change its functionality by exchanging the crosslinking points in response to some external stimuli (Figure 5-2). For example, in the case of polymer aqueous solution containing thermoresponsive polymer with Ru terpyridine (tpy) catalyst and pH-responsive polymer with thiol group, the addition of reductant will induce the reduction of Ru catalyst to $[Ru(tpy)_2]^{2+}$ and gelate the solution. Here, only the thermoresponsive polymers are crosslinked, so the gel will have only thermoresponsiveness. In contrast, the addition of oxidant will induce the oxidization of Ru catalyst to $[Ru(tpy)]^{3+}$, and form disulfide bond at the same time. The gel is now crosslinked only by disulfide bond of pH-responsive polymer, so the gel's property will be transformed from thermoresponsiveness to pH-responsiveness. The exchange of crosslinking points will be more effective by going through sol state, which has good analogy to the restructure of organs inside the pupal shell.

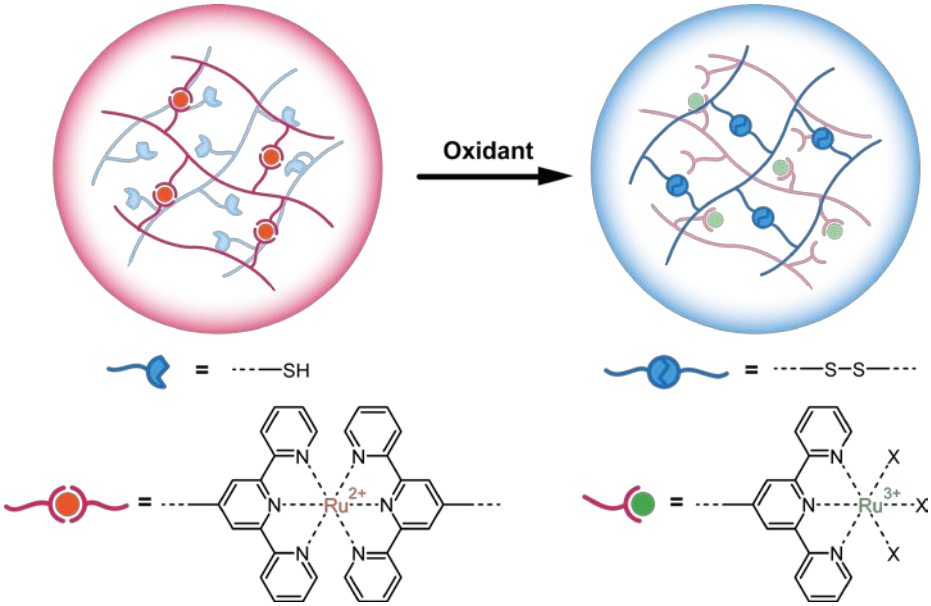

Figure 5-2. Schematic image of the functional gel which converts the crosslinking points in response to external stimuli (addition of oxidant) and transforms its functionality.

As mentioned above, the research about surface-grafted gels and further investigation to achieve artificial metamorphosis have potential to enhance the functionalities and the range of application of gels, and will help much deeper insight into various mysterious life phenomena.

5-3. References

[1] Plechkova, N. V.; Seddon, K. R. Applications of ionic liquids in the chemical industry. *Chem. Soc. Rev.* **2008**, *37*, 123-150.

[2] Ueki, T.; Watanabe, M. Polymers in Ionic Liquids: Down of Neoteric Solvents and Innovative Materials. *Bull. Chem. Soc. Jpn.* **2012**, *85*, 33-50.

Appendix

A. List of publications

Original papers (related to this dissertation)

1. **Ko Matsukawa**, Tsukuru Masuda, Aya Mizutani Akimoto, and Ryo Yoshida: "A surface-grafted thermoresponsive hydrogel in which the surface structure dominates the bulk properties", *Chem. Comm.* **2016**, *52*, 11064-11067. **[Highlighted on back cover]**

2. **Ko Matsukawa**, Tsukuru Masuda, Youn Soo Kim, Aya Mizutani Akimoto, and Ryo Yoshida; "Thermoresponsive surface-grafted gels: Controlling the "bulk" volume change properties by "surface" localized polymer grafting with various densities", *Langmuir* **2017**, 33, 13828-13833.

Original papers (others)

1. Erika Hasuike, Aya Mizutani Akimoto, Reiko Kuroda, **Ko Matsukawa**, Yuki Hiruta, Hideko Kanazawa, and Ryo Yoshida: "Reversible conformational changes in the parallel type G-quadruplex inside a thermoresponsive hydrogel", *Chem. Commun.* **2017**, *53*, 3142-3144.

2. Takeshi Ueki,* **Ko Matsukawa**,* Tsukuru Masuda, and Ryo Yoshida: "Protic Ionic Liquids for the Belousov-Zhabotinsky Reaction: Aspects of the BZ Reaction in Protic Ionic Liquids and Its Use for the Autonomous

Coil-Globule Oscillation of a Linear Polymer", *J. Phys. Chem. B* **2017**, *121*, 4592-4599. *Equally contributed to this work.

B. List of presentations

International conferences

1. ○**Ko Matsukawa**. Takeshi Ueki, and Ryo Yoshida: "BZ reaction using protic ionic liquid type self-oscillating gel", 22nd Polymer Networks Group Meeting and 10th Gel Symposium, The University of Tokyo, Tokyo, November 2014. (Poster)

2. ○**Ko Matsukawa**, Tsukuru Masuda, Aya Mizutani Akimoto, and Ryo Yoshida: "Preparation of the surface grafted hydrogel by ARGET ATRP", GelSympo2017, Nihon University, Chiba, March 2017. (Poster)

3. ○**Ko Matsukawa**, Tsukuru Masuda, Aya Mizutani Akimoto, and Ryo Yoshida: "Preparation of the hydrogel which has comb-type polymer network only in the surface region", IUMRS-ICAM 2017, Kyoto University, Kyoto, August 2017. (Oral) **[Langmuir Award]**

Domestic conferences

1. ○松川滉・上木岳士・吉田亮、「プロトン性イオン液体を用いた BZ 反応とイオン液体型自励振動ゲルへの展開」、第 62 回高分子学会年次大会、国立京都国際会館、2013 年 5 月（ポスター発表）

2. ○松川滉・上木岳士・吉田亮、「プロトン性イオン液体を用いた BZ 反応とイオン液体型自励振動ゲルへの展開」、第 62 回高分子討論会、金沢大学、2013 年 9 月（ポスター発表）

3. ○松川滉・上木岳士・吉田亮、「プロトン性イオン液体を用いた BZ 反応とイオン液体型自励振動ゲルへの展開」、ゲルワークショップ　イン加賀、ゆのくに天祥、2013 年 9 月（ポスター発表）

4. ○松川滉・上木岳士・吉田亮、「プロトン性イオン液体を用いた BZ 反応とイオン液体型自励振動高分子への展開」、第 4 回イオン液体討論会、慶應義塾大学、2013 年 11 月（ポスター発表）

5. ○松川滉・上木岳士・吉田亮、「プロトン性イオン液体を用いた化学振動反応とイオン液体型自励振動高分子への展開」、第 25 回高分子ゲル研究討論会、東京大学、2014 年 1 月（ポスター発表）**[優秀ポスター賞]**

6. ○松川滉・上木岳士・吉田亮、「プロトン性イオン液体型高分子を用いた BZ 反応」、第 63 回高分子学会年次大会、名古屋国際会議場、2014 年 5 月（ポスター発表）

7. ○上木岳士・**松川滉**・増田造・吉田亮、「プロトン性イオン液体を利用した BZ 反応の特性と自励振動高分子系への展開」、第 63 回高分子討論会、長崎大学、2014 年 9 月（口頭発表）

8. ○上木岳士・**松川滉**・増田造・吉田亮、「プロトン性イオン液体を利用した BZ 反応の特性」、第 5 回イオン液体討論会、横浜シンポジア、2014 年 10 月（口頭発表）

9. ○増田造・上木岳士・**松川滉**・吉田亮、「プロトン性イオン液体を用いた新規自励振動高分子系の構築」、第 5 回イオン液体討論会、横浜シンポジア、2014 年 10 月（ポスター発表）

10. ○上木岳士・**松川滉**・増田造・吉田亮、「プロトン性イオン液体を利用した BZ 反応の特性と自励振動高分子系への展開」、第 26 回高分子ゲル研究討論会、東京大学、2015 年 1 月（口頭発表）

11. ○増田造・上木岳士・**松川滉**・吉田亮、「プロトン性イオン液体を用いた新規自励振動高分子系の創製」、第 64 回高分子学会年次大会、札幌コンベンションセンター、2015 年 5 月（ポスター発表）

12. ○**松川滉**・増田造・秋元文・吉田亮、「ARGET-ATRP による表面グラフトハイドロゲルの創製」、第 64 回高分子討論会、東北大学、2015 年 9 月（ポスター発表）

13. ○増田造・上木岳士・玉手亮多・**松川滉**・吉田亮、「プロトン性イオン液体を利用した新規自励振動高分子系の創製と評価」、第 64 回高分子討論会、東北大学、2015 年 9 月（口頭発表）

14. ○増田造・上木岳士・玉手亮多・**松川滉**・吉田亮、「プロトン性イオン液体を利用する新規自励振動ゲルの設計」、第 6 回イオン液体討論会、同志社大学、2015 年 10 月（口頭発表）

15. ◯**松川滉**・増田造・秋元文・吉田亮、「表面近傍のみに高分子グラフト鎖が導入された温度応答性ハイドロゲルの創製」、第 37 回日本バイオマテリアル学会大会、京都テルサ、2015 年 11 月（ポスター発表）

16. ◯**松川滉**・増田造・秋元文・吉田亮、「Preparation of surface grafted hydrogels by ARGET ATRP」、第 25 回日本 MRS 年次大会、横浜市開港記念会館、2015 年 12 月（ポスター発表）**[奨励賞]**

17. ◯**松川滉**・増田造・秋元文・吉田亮、「バルク特性を支配する表面網目構造を持つ局在型グラフトゲルの創製」、第 27 回高分子ゲル研究討論会、東京大学、2016 年 1 月（ポスター発表）

18. ○増田造・上木岳士・玉手亮多・**松川滉**・吉田亮、「プロトン性イオン液体を利用した新規自励振動ゲルの創製」、第 27 回高分子ゲル研究討論会、東京大学、2016 年 1 月（ポスター発表）

19. ○松川滉・増田造・秋元文・吉田亮、「ARGET ATRP による表面局在型グラフトハイドロゲルの創製」、第 65 回高分子学会年次大会、神戸国際会議場、2016 年 5 月（口頭発表）

20. ○松川滉・増田造・秋元文・吉田亮、「表面近傍にのみ櫛型構造を有するハイドロゲルの調製および物性評価」、第 65 回高分子討論会、神奈川大学、2016 年 9 月（口頭発表）

21. ○松川滉・増田造・秋元文・吉田亮、「表面に櫛型グラフト構造を有するハイドロゲルの調製および物性評価」、第 28 回高分子ゲル研究討論会、東京大学、2017 年 1 月（口頭発表）

22. ○松川滉・増田造・秋元文・吉田亮、「密度の異なるグラフト鎖を有する表面グラフトゲルの調製および物性評価」、第 66 回高分子学会年次大会、幕張メッセ、2017 年 5 月（口頭発表）

23. ○松川滉・増田造・秋元文・吉田亮、「Analysis of surface and bulk properties of surface grafted gels depending on graft density」、第 66 回高分子討論会、愛媛大学、2017 年 9 月（口頭発表）

24. ○松川滉・増田造・秋元文・吉田亮、「グラフト密度に依存した表面グラフトゲルの表面物性およびバルク物性評価」、ゲルワークショップイン　松山、にぎたつ会館、2017 年 9 月（ポスター発表）

25. ○秋元文・田中信行・**松川滉**・春園嘉英・田中陽・吉田亮、「接触角では評価不能なハイドロゲル表面の精密濡れ性解析」、第 29 回高分子ゲル研究討論会、東京工業大学、2018 年 1 月（口頭発表）

26. ○古澤麻実・金娟秀・**松川滉**・秋元文・吉田亮、「LCST が異なるグラフト鎖を有する表面グラフトゲルの調製と自励振動ゲルへの展開」、第 29 回高分子ゲル研究討論会、東京工業大学、2018 年 1 月（ポスター発表）

C. Awards

1. 第 25 回高分子ゲル研究討論会　**優秀ポスター賞**　2014 年 1 月

2. 第 25 回日本 MRS 年次大会　**奨励賞**　2015 年 12 月

3. IUMRS-ICAM 2017　**Langmuir Award**　2017 年 8 月